



MONTCLAIR STATE
UNIVERSITY

Montclair State University
**Montclair State University Digital
Commons**

Theses, Dissertations and Culminating Projects

5-2018

Novel Bryophyte Auxin Conjugate Amidohydrolases from Physcomitrella patens and Marchantia polymorpha and Their Role in the Evolution of Auxin Metabolism

Stephanie Lyn Kurdach
Montclair State University

Follow this and additional works at: <https://digitalcommons.montclair.edu/etd>



Part of the [Biology Commons](#)

Recommended Citation

Kurdach, Stephanie Lyn, "Novel Bryophyte Auxin Conjugate Amidohydrolases from *Physcomitrella patens* and *Marchantia polymorpha* and Their Role in the Evolution of Auxin Metabolism" (2018). *Theses, Dissertations and Culminating Projects*. 137.
<https://digitalcommons.montclair.edu/etd/137>

This Thesis is brought to you for free and open access by Montclair State University Digital Commons. It has been accepted for inclusion in Theses, Dissertations and Culminating Projects by an authorized administrator of Montclair State University Digital Commons. For more information, please contact digitalcommons@montclair.edu.

Abstract

Auxin (indole-3-acetic acid) was the first phytohormone to be discovered, and today is still regarded as one of the most widely understood plant hormones. Auxin has the ability to stimulate, promote, delay, or inhibit many of a plant's physiological processes. The concentration of the hormone within a plant is critical; low concentrations of IAA positively impact plants' physiological processes, but high concentrations of IAA are inhibitory and toxic to plants. For this reason, auxin metabolism must be tightly regulated. Plants can regulate their endogenous concentration of auxin via conjugation to sugars, amino acids, or peptides. Indole-3-acetic acid is active when it is in its free state, and presumably inactive when it is in its conjugated form. Indole-3-acetic acid can exist in its inactive, conjugated form within a plant until it is needed, where it can then undergo hydrolysis from its conjugate via a hydrolase gene and become available for use within the plant. In an effort to better understand the IAA conjugation auxin metabolism strategy of plants, hydrolase genes have been identified, isolated, and studied in a variety of species. Hydrolases are enzymes that cleave the bond between IAA and its amide or ester conjugate, thereby releasing free active auxin that is available for use within the plant. Given the conservation of auxin regulation metabolism, we have become interested in investigating the conservation of hydrolase genes. Hydrolase genes have been identified in numerous tracheophyte species, but we are interested in tracing these genes as far back as possible in evolutionary time. We have isolated, characterized the enzymatic activity, and investigated the evolutionary implications of several newly identified bryophyte hydrolases from the moss species *Physcomitrella patens* and the liverwort species *Marchantia polymorpha*.

MONTCLAIR STATE UNIVERSITY

Novel bryophyte auxin conjugate amidohydrolases from *Physcomitrella patens* and *Marchantia polymorpha* and their role in the evolution of auxin metabolism

by

Stephanie Lyn Kurdach

A Master's Thesis Submitted to the Faculty of

Montclair State University

In Partial Fulfillment of the Requirements


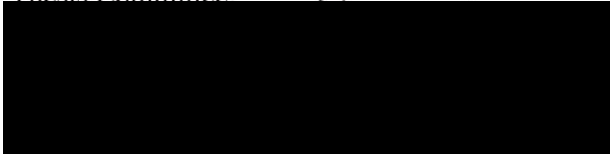
For the Degree of

Master of Science in Molecular Biology

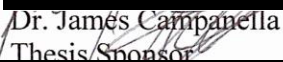
May 2018

College/School College of Science
and Mathematics

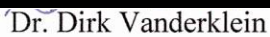
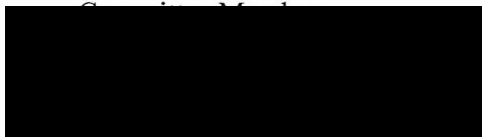
Department Biology

Thesis Committee:



Dr. James Campanella
Thesis Sponsor




Dr. Dirk Vanderklein

Dr. Scott Kight
Committee Member

NOVEL BRYOPHYTE AUXIN CONJUGATE AMIDOHYDROLASES
FROM *PHYSCOMITRELLA PATENS* AND *MARCHANTIA*
POLYMORPHA AND THEIR ROLE IN THE
EVOLUTION OF AUXIN
METABOLISM

A THESIS

Submitted in partial fulfillment of the requirements
For the degree of Master of Science in Molecular Biology

by

STEPHANIE LYN KURDACH

Montclair State University

Montclair, NJ

2018

Copyright © 2018 by *Stephanie Lyn Kurdach*. All rights reserved.

Acknowledgements

I would like to express my gratitude to those who have mentored me throughout my research and academic career at Montclair State University.

Dr. James Campanella, *Thesis Advisor*
Dr. Scott Kight, *Thesis Committee*
Dr. Dirk Vanderklein, *Thesis Committee*

Lastly, thank you to all of the faculty members who taught me and worked with me during my academic career at Montclair State University. I owe much of my academic success to your words of encouragement and motivation.

Table of Contents	Page
Abstract.....	i
Signature Page.....	ii
Title Page.....	iii
Copyright.....	iv
Acknowledgements.....	v
List of Figures.....	vii
Thesis.....	1
Introduction.....	1
Materials and Methods.....	17
Results.....	30
Moss Results.....	30
Liverwort Results.....	34
Discussion.....	40
Moss Discussion.....	40
Liverwort Discussion.....	44
Bibliography.....	49
Tables.....	59
Figure Legends.....	62
Figures.....	64

List of Tables	Page
Table 1. Newly identified bryophyte hydrolases.....	59
Table 2. Genomic DNA extraction from moss PCR primers.....	59
Table 3. Protocol specifications for endonuclease digests.....	59
Table 4. Amino acid similarity matrix.....	60
Table 5. Quantification of hydrolase activity.....	61
Table 6. Hydrolase copy number comparison.....	61

List of Figures	Page
Figure 1. Auxin chemical structures.....	64
Figure 2. Sztein et al. (2000) theoretical cladogram.....	64
Figure 3. Construction of hydrolase inserts into expression vectors.....	65
Figure 4. Phylogenetic analyses.....	67
Figure 5. Principal coordinate analysis based on codon usage.....	69
Figure 6. Gel electrophoresis analysis of extracted moss DNA.....	72
Figure 7. Endonuclease digests.....	74
Figure 8. High pressure liquid chromatography (HPLC) sample.....	77
Figure 9. M20D conserved metallopeptidase domains.....	77
Figure 10. Proposed cladogram.....	78
Figure 11. Liverwort hydrolase structures.....	78

Introduction

Phytohormones are the chemicals found in plants that are responsible for the regulation of many of the plants' physiological processes. Auxin was the first phytohormone to be discovered, and today is still regarded as one of the most widely understood plant hormones. Auxin's discovery was due in part to the work of Charles Darwin (1880). His experimentation involved exposing the tips of radicles to different conditions, such as physical damage, pressure, air moisture, light, and gravity (Darwin 1880). Exposure to each of these conditions yielded movement from the radicle; whether the movement was towards the condition or away from it, it was always at the advantage of the plant. This experimentation showed that plants do have sensory perception—roots act as a “brain” for the plant (Darwin 1880).

Sensory perception was studied in plants by tracking the phytohormone's movement, and isolating the hormone for further study (Fitting 1907; Boysen-Jensen 1913; Paal 1918; Soding 1925; Went 1926, 1928). The first “*Avena* curvature test” involved cutting the coleoptile tips off of plants, and then placing them onto agar blocks. After some time, the agar blocks were placed onto *Avena sativa* stems where the coleoptile had been cut off. The placement of the agar block onto the *A. sativa* stem caused the stem to resume growth (Went 1926). The curvature that occurred in the stems was proportional to the amount of the hormone that diffused through the agar block (Went 1928).

Indole-3-acetic acid (IAA) was discovered in fermentation media before it was discovered in plant tissues and associated with auxin (Salkowski 1885). The first compounds which were isolated and named “auxin” came from human urine (Kögl and

Haagen-Smit 1931; Kögl et al. 1934b). Shortly after, the same auxin compound was isolated from the fungus *Rhizopus suinus* (Thimann 1935). Auxin is represented by several different chemical structures, but the most prominent is indole-3-acetic acid (Kögl et al. 1934a; Thimann and Koepfli 1935). The structure of indole-3-acetic acid ($C_{10}H_9NO_2$) is represented by an indole ring with an attached carboxymethyl group (Fig. 1a) (Koepfli et al. 1938). The first plant from which auxin (IAA) was isolated and identified was maize, *Zea mays* (Haagen-Smit et al. 1946).

Auxin can be found in all plants, although the concentration within each plant differs. Auxin has the ability to stimulate, promote, delay, or inhibit many of a plant's physiological processes (Davies 1995; Mauseth 1991; Raven 1992; Salisbury and Ross 1992). Specifically, auxin has been found to stimulate cell elongation, cell division, cell differentiation between the xylem and phloem, root initiation, the growth of flowering organs, gravitropism, phototropism, and the production of the phytohormone ethylene. Auxin can also promote abscission, flowering, and fruit growth in certain species. In contrast, auxin can delay processes such as leaf senescence and fruit ripening, and inhibit processes such as abscission, and the growth of lateral buds (Davies 1995; Mauseth 1991; Raven 1992; Salisbury and Ross 1992).

The evolution of modern terrestrial plants can all be traced back to a common algal ancestor 500 million years ago (Lewis and McCourt 2004; Leliaert et al. 2012; Timme et al. 2012). The charophycean green algae presumably gave way to the earliest land plants (bryophytes), followed by modern land plants (tracheophytes) (Graham 1993; Gray 1993; Strother et al. 1996). Bryophytes are spore-forming, non-vascular land plants that include liverworts, hornworts, and mosses. Tracheophytes are spore-producing, or

seed-containing vascular plants. Spore-producing vascular plants, such as ferns, evolved first. Seed-containing vascular plants, including all gymnosperms and angiosperms, eventually followed. The evolution of modern terrestrial seed-containing plants from bryophytes occurred over 450 million years ago (Theissen et al. 2001).

The evolution of these first land plants occurred during the Ordovician Period, around 485-443 million years ago (Graham 1993; Gray 1993; Strother et al. 1996). The establishment of land plants changed the Earth's atmosphere, as well as the genome of all plants to come (Parnell and Foster 2012; Scott and Glasspool 2006; Rensing et al. 2008; Hori et al. 2014). While colonizing land, the first terrestrial plants enlarged their body size, adapted to drought, high intensity light, and UV radiation (Rensing et al. 2008; Hori et al. 2014; Campanella et al. 2014a). *Klebsormidium flaccidum* is a charophytic, terrestrial algae that contains several genes and hormones specific to land plants, including auxin. Genome analysis of *K. flaccidum* shows that it was likely an early transition from charophytes to bryophytes (Hori et al. 2014). The presence of auxin receptor, sensing, and transport genes in *K. flaccidum* suggests that auxin metabolism in plants is an ancient, conserved process (Hori et al. 2014; Cooke et al. 2002).

Auxin metabolism is regulated by four main processes: biosynthesis, transport, conjugation, and degradation (Normanly et al. 1995; Normanly and Bartel 1999; Ljung et al. 2002). The concentration of IAA in a plant is critical; low concentrations of IAA positively impact plants' physiological processes, but high concentrations of IAA are inhibitory and toxic to plants (Bandurski et al. 1995). For this reason, auxin metabolism must be tightly regulated. Auxin biosynthesis allows a plant to increase its endogenous auxin concentration. Auxin biosynthesis can occur via tryptophan (Trp)-dependent

pathways or Trp-independent pathways (Nonhebel et al. 1993). The Trp-dependent pathways include the IAOx pathway, IAM pathway, and IPyA pathway—all named after IAA intermediates (Korasick et al. 2013). Although many of the specific enzymes and intermediates within the pathways are still unclear, the Trp-dependent pathways generally begin with tryptophan as the origin of the indole ring, which is then converted into an intermediate such as indole-3-acetaldoxime (IAOx), indoleacetamide (IAM), or indole-3-pyruvic acid (IPyA), and is lastly converted into IAA (Sztein et al. 2000; Zhao et al. 2002; Sugawara et al. 2009; Pollmann et al. 2003; Stepanova et al. 2008, 2011; Tao et al. 2008; Mashiguchi et al. 2011; Won et al. 2011). The Trp-independent pathways are less understood, but generally begin with an indole ring that is eventually converted into IAA (Sztein et al. 2000; Ouyang et al. 2000).

After the biosynthesis of auxin occurs, the concentration of the hormone within the plant must be tightly regulated. If too much auxin is present, degradation will occur. Indole-3-acetic acid catabolism is an oxidative process. Indole-3-acetic acid can be degraded by a decarboxylative pathway in which the acetic acid side chain is oxidized, or by a non-decarboxylative pathway in which the indole ring is oxidized (Normanly et al. 1995; Slovin et al. 1999). There are, however, two ways that a plant can regulate its endogenous concentration of auxin, without degrading the hormone. First, auxin can be transported away from the site of biosynthesis via PIN-FORMED (PIN) proteins (Friml et al. 2003; Ludwig-Müller 2009). PIN-FORMED proteins are responsible for transporting auxin from cell to cell. This polar transport creates an apical-basal auxin gradient within the plant, thereby maintaining auxin homeostasis (Friml et al. 2003). A

plant can also regulate its endogenous concentration of auxin via conjugation to sugars, amino acids, or peptides (Zenk et al. 1961; Feung et al. 1976, 1977).

Indole-3-acetic acid is active when it is in its free state, and presumably inactive when it is in its conjugated form. Amide-bound conjugates form when indole-3-acetic acid binds with amino acids, small peptides, or small proteins. Ester-bound conjugates form when indole-3-acetic acid binds with small sugars, polysaccharides, inositol, or glycoproteins (Sztein et al. 2000). The conjugated form of IAA is a “short-term intermediate” in the regulation of IAA metabolism (Cohen and Bandurski 1982; Kleczowski and Schell 1995). Indole-3-acetic acid can exist in its inactive, conjugated form within a plant until it is needed, where it can then undergo hydrolysis from its conjugate via a hydrolase gene and become available for use within the plant.

Different conjugates have been identified to have different functions within plants. Further, different plants have different preferred conjugate forms. Ester-bound conjugates, for example, are present in many tracheophytes and bryophytes, but they are the predominant conjugate form in *Zea mays* (Sztein et al. 1999; Bandurski et al. 1995). Conjugates such as IAA-glucose and IAA-*myo*-inositol have been identified in *Z. mays*, and both serve as auxin storage forms (Cohen and Bandurski 1982; Nicholls 1967; Chisnell 1984). Similarly, amide-bound conjugates have been identified in many tracheophytes, bryophytes, and charophytes (Sztein et al. 1999, 2000). Amide-bound conjugates are the preferred form for tracheophytes and bryophytes (Sztein et al. 1999, 2000). Conjugates such as IAA-Alanine, IAA-Aspartate, IAA-Glutamate, IAA-Glycine, IAA-Glutamine, IAA-Leucine, IAA-Phenylalanine, IAA-Tryptophan, and IAA-Valine have been identified and studied for their function (Korasick et al. 2013).

The conjugates IAA-Alanine and IAA-Leucine serve as auxin storage forms in several different plant species (Korasick et al. 2013). Within the dicot, *Arabidopsis thaliana*, IAA-Alanine and IAA-Leucine both readily undergo hydrolysis, and provide active IAA for use within the plant (Bartel and Fink 1995; Rampey et al. 2004). IAA-Alanine and IAA-Leucine are also responsible for inhibiting root elongation in *A. thaliana* (LeClere et al. 2002). On the other hand, IAA-Aspartate and IAA-Glutamate do not readily undergo hydrolysis in *A. thaliana*, therefore, they do not provide the plant with active IAA, and likely serve as intermediates in the inactivation process of auxin (Östin et al. 1998; LeClere et al. 2002; Rampey et al. 2004; Korasick et al. 2013). In *Medicago truncatula*, IAA-Aspartate does readily undergo hydrolysis and provide active IAA for use within the plant—providing evidence that amide conjugates can have different functions within different species (Campanella et al. 2008). The conjugate IAA-tryptophan inhibits plant growth within *A. thaliana*, and is categorized as an “antagonist” (Staswick 2009). The specific roles for IAA-Glycine, IAA-Glutamine, IAA-Phenylalanine, and IAA-Valine are still unclear (Korasick et al. 2013).

Indole-3-butyric acid (IBA) and indole-3-propionic acid (IPA) are two other endogenous auxins that also exist within plants (Blommaert 1954; Linser et al. 1954; Bayer 1969) (Fig. 1b, c). Similar to IAA, IBA and IPA can exist in a free state, or in a conjugated form (Andreae and Good 1957; Tabone and Tabone 1953; Tabone 1958). Indole-3-butyric acid can form both amide and ester-bound conjugates, including IBA-Alanine, IBA-Glycine, IBA-Glutamate, and IBA-glucose (Woodward and Bartel 2005; Bajguz and Piotrowska 2009; Ludwig-Müller 2011). Indole-3-propionic acid, on the other hand, is less understood. The only IPA conjugate that has been extensively studied

in plants is IPA-Alanine, yet it remains unknown if this is a naturally occurring substrate (Campanella et al. 2004; Savić et al. 2009). The specific purpose of IBA and IPA conjugates within plants is still unclear, however, there have been instances in which these conjugates were preferentially employed by plants over IAA conjugates (Korasick et al. 2013). In the wheat species, *Triticum aestivum*, IBA and IPA conjugates are physiologically preferred over IAA conjugates (Campanella et al. 2004). Likewise, in *Brassica rapa*, IPA conjugates are preferred over IAA conjugates (Savić et al. 2009).

The concentration of free IAA versus conjugated IAA can differ significantly in different plant species. In tracheophytes, up to 90% of the plants' total IAA composition is stored as conjugates (Sztein et al. 1999, 2000). Mosses also have approximately 90% of the plants' total IAA composition stored as conjugates (Sztein et al. 1999). In liverworts and green algae, however, IAA conjugates only reach up to about 70% of the plant's total IAA composition (Sztein et al. 1999, 2000). This is evidence that different plant species have adopted different metabolic pathways to maintain auxin homeostasis.

Endogenous auxin has been discovered in every major plant group, including tracheophytes, bryophytes, and algae (Stirk et al. 2013). Endogenous auxin has also been found in species as old as eubacteria and archaeobacteria (Maruyama et al. 1989; Lee et al. 2004; White 1987). The auxin metabolism of many of these species has been characterized. Bacteria typically produce IAA through the Trp-dependent biosynthetic pathways; intermediates include indole-3-pyruvate (IPyA), indole-3-acetamide (IAM), and tryptamine (TAM) (Spaepen and Vanderleyden 2011). The IAM pathway has been identified in the bacteria *Pseudomonas savastanoi*, and species from the bacterial genera *Agrobacterium*, *Erwinia*, and *Azospirillum* (Lambrecht et al. 2000). Likewise, the IPyA

pathway has been identified in *Pantoea agglomerans* and *Enterobacter cloacae*, as well as species from the genera *Azospirillum*, *Bacillus*, *Bradyrhizobium*, *Paenibacillus*, *Pseudomonas*, and *Rhizobium* (Spaepen and Vanderleyden 2011). The IPyA pathway utilizes TAA and YUC proteins to synthesize IAA, and it has been speculated that these proteins may have arisen in land plants from horizontal gene transfer events from bacteria (Yue et al. 2014).

Bacteria have the ability to regulate auxin metabolism via IAA conjugation and hydrolysis. Conjugation has been identified in *P. savastanoi*, in which IAA binds with the amino acid lysine (Romano et al. 1991; Spena et al. 1991). Likewise, hydrolysis from the IAA-Aspartate conjugate has been identified in *Enterobacter agglomerans* (Chou et al. 1998). It still remains unclear exactly why bacteria have the ability to regulate auxin in a similar fashion as plants, but one theory hypothesizes that it may be because soil bacteria have evolved in close proximity to plants, leading to symbiotic evolution and a mutualistic relationship (Ludwig-Müller 2011). Ludwig-Müller (2011) speculates that pathogenic bacteria living inside of plants aid in IAA conjugation. The bacteria will form IAA conjugates that the plant cannot hydrolyze into free active IAA, thereby causing the plant to maintain its auxin levels through “detoxification” (Ludwig-Müller 2011). The bacteria spare the plant from accumulating an overabundance of auxin, and therefore the healthy plant is able to provide nutrients for the bacteria. On the other hand, free-living rhizosphere bacteria aid the plants in IAA-conjugate hydrolysis (Ludwig-Müller 2011). The free-living bacteria will hydrolyze IAA conjugates thereby giving the plant free active IAA. This will stimulate root growth for the plant, and allow the bacteria to obtain more nutrients from the soil (Ludwig-Müller 2011). The plant is able to maintain its

endogenous auxin levels, and the bacteria are able to live off of the plant and soil around it. Although little is known about the auxin metabolism of bacteria, it is clear that a relationship does exist between the auxin metabolism of bacteria and land plants.

Microalgae are microscopic, unicellular algae. The auxin metabolism has been investigated in microalgal strains from the classes Chlorophyceae, Trebouxiophyceae, Ulvophyceae, and Charophyceae—all classes of green algal species (Stirk et al. 2013). Stirk et al. (2013) examined 24 different microalgal species. All of the species contained auxin in the form of IAA and IAM (Stirk et al. 2013). It is likely that microalgae synthesize IAA via the Trp-dependent IAM biosynthetic pathway (Jirásková et al. 2009; Stirk et al. 2013). Microalgae do not regulate their endogenous auxin levels via conjugation, given that the only IAA “conjugate” identified was IAM (Stirk et al. 2013). Rather, the purpose of the high auxin levels is likely due to regulation of cell growth and division (Stirk et al. 2013). Other multicellular algae that have been studied for their auxin metabolism come from the *Nitella* genus of charophytes (Sztein et al. 2000). The endogenous auxin composition of *Nitella* is almost evenly divided among free IAA (28%), IAA-ester conjugates (34%), and IAA-amide conjugates (38%) (Sztein et al. 2000). It has been speculated that algae may have an easier time regulating their free IAA levels than land plants do, because they are surrounded by water and can easily secrete unwanted compounds into the water around them for dissolution (Ludwig-Müller 2011). Further, given the slow rate of conjugation synthesis, it is likely that charophytes do not use conjugation to regulate their endogenous auxin levels (Sztein et al. 2000). Instead, charophytes likely regulate their endogenous auxin levels via IAA biosynthesis and degradation (Sztein et al. 2000).

Bryophytes that have been studied for their auxin metabolism include liverworts, hornworts, and mosses (Sztein et al. 1999, 2000). Liverwort species such as *Marchantia polymorpha*, *Pallavicinia lyellii*, *Reboulia hemisphaerica*, *Sphaerocarpos texanus*, and the genus *Plagiochila*, have been studied and characterized (Sztein et al. 1999, 2000). The majority of the liverworts' IAA composition is in the form of IAA-amide conjugates (52%), but IAA-ester conjugates (20%) and free IAA (28%) were also identified (Sztein et al. 1999). The auxin metabolism of liverworts is similar to that of charophytes; conjugation occurs at a slow rate, therefore, liverworts likely regulate their endogenous auxin levels via IAA biosynthesis and degradation (Sztein et al. 1999). The hornwort *Phaeoceros laevis* has also been studied for its auxin metabolism (Sztein et al. 2000). The majority of *P. laevis*' IAA composition is in the form of IAA-amide conjugates (82%), but IAA-ester conjugates (7%) and free IAA (11%) were also identified within its auxin composition (Sztein et al. 2000). Upon exposure to exogenous IAA, the hornwort was able to rapidly conjugate over 50% of the IAA, suggesting that hornworts regulate their endogenous auxin levels via IAA conjugation (Sztein et al. 2000). Moss species such as *Funaria hygrometrica*, *Polytrichum ohioense*, *Sphagnum angustifolium*, and *Orthotrichum lyellii* have also been studied for their auxin composition and metabolism (Sztein et al. 1999). Similar to hornwort, IAA-amide conjugates dominate the total IAA composition (85%), and only a minor amount of IAA-ester conjugates (5%) and free IAA (10%) exists (Sztein et al. 1999). Exposure to exogenous IAA also rapidly produces conjugates within the mosses, suggesting that their auxin metabolism is regulated via IAA conjugation (Sztein et al. 1999, 2000).

Two tracheophytes that have been studied to elucidate auxin metabolism include the fern, *Ceratopteris richardii*, and the clubmoss, *Selaginella kraussiana* (Sztein et al. 1999, 2000). The IAA composition of both species showed a preference for IAA-amide conjugates, and a relatively small amount of free IAA. The IAA composition of *C. richardii* contained IAA-amide conjugates (77%), IAA-ester conjugates (1%), and free IAA (22%) (Sztein et al. 1999). Likewise, the IAA composition of *S. kraussiana* contained IAA-amide conjugates (75%), IAA-ester conjugates (16%), and free IAA (9%) (Sztein et al. 1999). Both species were exposed to exogenous IAA, and conjugation rapidly occurred (Sztein et al. 1999). This evidence suggests that tracheophytes regulate their auxin metabolism via IAA conjugation (Sztein et al. 1999, 2000).

Auxin metabolism is generally classified into two main strategies—IAA biosynthesis and degradation, or IAA conjugation (Sztein et al. 1999, 2000). Evolutionarily, the charophytes evolved first, followed by the bryophytes, and finally the tracheophytes. The charophytes have relatively high levels of free IAA and conjugation occurs slowly, if at all. The charophytes, therefore, employ the IAA biosynthesis and degradation strategy to regulate auxin metabolism (Sztein et al. 1999, 2000). The biosynthesis/degradation strategy may be the “ancestral” form of auxin regulation (Sztein et al. 2000). The charophytes gave way to the bryophytes—the first terrestrial plants—with little change in auxin metabolism and regulation. Although liverworts contain IAA conjugates, conjugation still occurs at a very slow rate. Sztein et al. (1999, 2000) concluded that liverworts also employ the IAA biosynthesis and degradation strategy to regulate auxin metabolism.

The later hornworts, mosses, and tracheophytes are all similar in terms of auxin metabolism. All three groups of plants contain high levels of IAA conjugates, low levels of free IAA, and conjugation occurs at rapid rates. Hornworts, mosses, and tracheophytes all employ the IAA conjugation strategy for auxin metabolism (Sztein et al. 1999, 2000). Although the exact timeline for the evolution of auxin regulation is unclear, sometime during the evolution of bryophytes, auxin regulation metabolism changed. Sztein et al. (2000) suggests a theoretical cladogram that defines the evolution of auxin metabolism (Fig. 2). Early auxin metabolism begins with the IAA biosynthesis/degradation strategy in charophytes and liverworts, and evolves into the IAA conjugation strategy in hornworts, mosses, and vascular plants, respectively (Sztein et al. 2000). This theoretical cladogram leaves room for future development in terms of the evolution of auxin metabolism, and the relationship between auxin metabolism strategy and the development of different plant species.

In an effort to better understand the IAA conjugation auxin metabolism strategy of plants, hydrolase genes have been identified, isolated, and studied in a variety of species. Hydrolases are enzymes that cleave the bond between IAA and its amide or ester conjugate, thereby releasing free active auxin that is available for use within the plant (Bartel and Fink 1995). Auxin amidohydrolases—hydrolase enzymes that specifically cleave auxin from an amino acid conjugate—were first identified using “mutant screens” (Bartel and Fink 1995; Ludwig-Müller 2011). If a wild-type plant is exposed to exogenous IAA conjugates, functional hydrolases will cleave the conjugates and expose the plant to free active IAA. An overabundance of this free IAA will accumulate in the plant, inhibiting its growth and possibly killing it. If a mutant plant is exposed to

exogenous IAA conjugates, mutant hydrolases will not be able to cleave the conjugates. No free IAA will accumulate within the plant, and “normal” growth will occur (Bartel and Fink 1995; Davies et al. 1999; Rampey et al. 2004). These mutant screens can be performed on living plants to identify mutant hydrolase genes based upon the presence or absence of plant growth (Savić et al. 2009). Mutant hydrolases were named after the IAA conjugate that could not be cleaved.

The first mutant screens were performed in *Arabidopsis thaliana*, and three different classes of amidohydrolases were identified. The three major classes of amidohydrolases are IAA-LEUCINE RESISTANT1 (ILR1) hydrolases, ILR1-LIKE1 (ILL1) hydrolases which are paralogs of ILR1 hydrolases, and IAA-ALANINE RESISTANT3 (IAR3) hydrolases (Bartel and Fink 1995; LeClere et al. 2002; Davies et al. 1999). In order for hydrolase homologs to be identified in other species, the complete genome of a given species must be available. Although this is a limiting factor, amidohydrolases have been identified in various tracheophyte species including *Arabidopsis thaliana* (AtILR1, AtILL1, AtILL2, AtILL3, AtILL5, AtILL6, AtIAR3), *Arabidopsis suecica* (AsILR1), *Triticum aestivum* (TaIAR3), *Populus euphratica* (PeILL3), *Populus × canescens* (PcILL3), *Medicago truncatula* (MtIAR31, MtIAR32, MtIAR33, MtIAR34, MtIAR36) *Brassica rapa* (BrIAR3, BrILL2), *Picea sitchensis* (PsIAR31, PsIAR32, PsIAR33, PsIAR34, PsIAR35), and *Pinus taeda* (PtIAR31, PtIAR32, PtIAR33, PtIAR34, PtIAR35) (Bartel and Fink 1995; Davies et al. 1999; LeClere et al. 2002; Sanchez Carranza et al. 2016; Campanella et al. 2003b, 2004; Junghans et al. 2006; Campanella et al. 2008; Savić et al. 2009; Campanella et al. 2011, 2014b).

Given the conservation of auxin regulation metabolism, we have become interested in investigating the conservation of hydrolase genes. Hydrolase genes have been identified in numerous tracheophyte species, but we are interested in tracing these genes as far back as possible in evolutionary time. Campanella et al. (2003b, 2004, 2008, 2011, 2014b) began this project over a decade ago with the identification of hydrolase genes in other tracheophyte species. They identified hydrolase genes in *Arabidopsis suecica*, *Triticum aestivum*, *Medicago truncatula*, *Picea sitchensis*, and *Pinus taeda*. They also studied the conservation of hydrolases in dicots such as potato, tomato, soybean, grape, and lotus, and monocots such as corn, rice, and barley (Campanella et al. 2003a). In an effort to further investigate the evolutionary conservation of these hydrolase genes, they began to explore bryophyte species.

Ludwig-Müller et al. (2009) speculated that the moss species, *Physcomitrella patens*, is a “dead end” in terms of auxin conjugate hydrolysis. An analysis of the *P. patens* genome by Ludwig-Müller et al. (2009) did not yield any hydrolase homologs, suggesting that conjugation cannot be reversed in these early plant species. Instead, Ludwig-Müller et al. (2009) proposed that auxin conjugation may occur as an intermediate in auxin inactivation, and hydrolase genes evolved in later species. It was suggested that additional bryophyte genomes are needed to further validate this claim. According to Ludwig-Müller et al. (2009), it was questionable whether only *P. patens* lacks hydrolases and the ability to properly use conjugation as a means of auxin metabolism or if this was true for all bryophyte species.

On the contrary, we performed our own analysis of the *P. patens* genome and identified several IAR3 hydrolase homologs (Table 1) (Kurdach et al. 2017). Further

experimentation was done to analyze these hydrolases. We isolated and characterized the hydrolases in terms of auxin conjugate activity and substrate recognition, and we revealed that some are functional within *P. patens*. This prompted us to search back even further to the most ancient extant land plant that evolved approximately 475 million years ago—liverwort (Wellman et al. 2003). We performed a genome search analysis of *Marchantia polymorpha*, because a new version of the DNA sequence became available in 2016 (v3.1). Again, we were able to identify one ILR1 hydrolase homolog (Table 1). Using this data, we isolated and characterized this liverwort hydrolase to determine whether or not it is functional, and the extent of its activity on auxin conjugates and substrate recognition. We performed these experiments to trace amidohydrolase genes evolutionarily as far back as possible. We hypothesized that because we were able to identify several homologous bryophyte hydrolase genes, we would be able to detect similar functions to those previously isolated tracheophyte hydrolases.

Another major question that we have become interested in investigating involves analyzing the evolutionary changes of auxin amidohydrolase genes. Presumably, these hydrolase genes are highly conserved among many species (Campanella et al. 2003a). Our goal was to uncover how these hydrolases may have changed over evolutionary time. There are several factors that can be examined to study how hydrolases may have changed over time. The first is to study the DNA and protein sequences of hydrolase homologs. From this data, any molecular changes in the sequence and structure of hydrolase homologs over evolutionary time can be identified. Further, the activity of the hydrolases can also be analyzed. Specifically, enzymatic activity can be analyzed for any changes, including changes in substrate specificity for certain conjugates. Potentially

redundant families of paralogous hydrolase genes within species can also be analyzed. For example, *Arabidopsis thaliana* has a redundant family of seven hydrolase genes (AtILR1, AtILL1, AtILL2, AtILL3, AtILL5, AtILL6 and AtIAR3) (Bartel and Fink 1995; LeClere et al. 2002; Davies et al. 1999). An analysis of more ancient species, particularly bryophytes, can be performed to determine if redundant families exist as well, or if more ancient species have fewer hydrolase genes. This analysis allows us to examine the correlation between the evolution and multiplicity of hydrolases among different species. To investigate the evolutionary changes of hydrolase genes, we compared the sequences, enzymatic activity, and number of hydrolases from different plant species. We hypothesized that identifiable evolutionary changes would be correlated with changes in hydrolase function. In other words, the newly identified moss and liverwort hydrolases would carry evolutionary molecular changes if the function of the hydrolases was different from previously identified tracheophyte hydrolase genes. On the other hand, we hypothesized that if the function of the moss and liverwort hydrolase genes was the same as previously identified tracheophyte hydrolase genes, the newly characterized genes would not have any major molecular changes and evolutionary change would not be easily identifiable.

Materials and Methods

Initial identification of homologs

A previous analysis of the *Physcomitrella patens* genome identified four hydrolase homologs—PpIAR31, PpIAR32, PpIAR33, and PpIAR34 (Skibitski 2016). The analysis was performed through a BLAST search of the *P. patens* genome (v3.3) using the AtIAR3 hydrolase homolog (www.phytozome.jgi.doe.gov).

A similar BLAST analysis of the *Marchantia polymorpha* genome (v3.1) was performed (www.phytozome.jgi.doe.gov). The PsIAR3 homolog of Sitka spruce was employed as a search probe in the BLAST analysis, and one *M. polymorpha* hydrolase homolog was identified. An NCBI protein BLAST search with the newly identified liverwort hydrolase showed that it was more similar to ILR hydrolases than IAR hydrolases—hence it was named MpILR1. BLAST analyses were performed with default search parameters.

Genomic DNA extraction from moss and PCR analysis

The moss genomic DNA extraction procedure employed approximately 30 mg of dried *P. patens* tissue (donated by Jutta Ludwig- Müller, University of Dresden). Extraction was performed with the QIAGEN DNeasy Plant Mini Kit (QIAGEN, Hilden, Germany). Tissue was ground using a mortar and pestle with 800 µl of “AP1” buffer (QIAGEN proprietary formula) and 3 µl of RNase. This mixture was transferred to a 2 ml microfuge tube, incubated at 65°C for 10 min, and mixed by hand three times during the incubation. Next, 130 µl of “AP2” (renamed by QIAGEN “P3” in 2012) buffer (3.0 M potassium acetate, pH 5.5) was added, mixed, and incubated for 10 min on ice. Following

incubation, the mixture was centrifuged for 2 min at 13,400 rpm. The flow-through was measured and transferred into a new 1.5 ml microfuge tube. The amount of “AP3” (renamed by QIAGEN “AW1” in 2012) buffer (0.5x; QIAGEN proprietary formula) and 100% ethanol (1x) needed were determined by the flow-through volume (1x). After mixing well, we added 650 μ l of the extract to the DNeasy column and centrifuged it for 1 min at 8,000 rpm. We discarded the flow-through and repeated the centrifugation with any remaining extract. Next, we added 500 μ l of “AW” (renamed by QIAGEN “AW2” in 2012) wash buffer (300 μ l “AW” stock buffer [QIAGEN proprietary formula], 700 μ l EtOH) to the column, centrifuged it for 1 min at 8,000 rpm, and discarded the flow-through. We repeated the wash with another 500 μ l aliquot of “AW” buffer, centrifuged the column for 2 min at 13,400 rpm, and discarded any flow-through. Another centrifugation was done for 1 min at 13,400 rpm to remove any remaining ethanol. We then placed the DNeasy column onto a new 1.5 ml microfuge tube and added 70 μ l of 65°C sterile water to the column. We incubated the column for 5 min at room temperature and centrifuged the tube one final time for 1 min at 8,000 rpm. The extracted DNA was stored at -20°C.

This DNA extraction procedure was repeated to obtain a second sample of the moss genomic DNA. The concentration of the two moss genomic DNA samples was 6.0 ng/ μ l and 4.9 ng/ μ l, respectively. These values were determined using a NanoDrop ND-1000 Spectrophotometer (Thermo Fisher Scientific Inc., Waltham, Massachusetts).

Both samples of moss genomic DNA underwent PCR to detect each of the four moss hydrolase homologs (PpIAR31-34). Four reaction tubes were set up for each of the hydrolases. Tube 1 contained 5 μ l of moss sample 1 DNA, 1 μ l of each appropriate

primer (Table 2), 12.5 μ l of Mastermix (Denville Scientific Inc., Holliston, Massachusetts), and 5.5 μ l of sterile DI water—equaling a total volume of 25 μ l. Tube 2 was a control for moss sample 1 and contained 5 μ l of moss sample 1 DNA, 1 μ l of universal 18S primers (QuantumRNA Classic II 18S Internal Standard, Thermo Fisher Scientific Inc., Waltham, Massachusetts), 12.5 μ l of Mastermix, and 6.5 μ l of sterile DI water. Tube 3 had the same contents as tube 1, except 5 μ l of moss sample 2 DNA was used. Tube 4 had the same contents as tube 2, except 5 μ l of moss sample 2 DNA was used. All primers were constructed by Invitrogen (a division of Thermo Fisher Scientific Inc., Waltham, Massachusetts) and were resuspended in 1 ml of sterile DI water before being added to our reaction tubes. When preparing the PCR tubes, we added the DNA, water, and primers to the reaction tubes first. Then we incubated the tubes in the thermocycler for 1 min at 95°C (Eppendorf Mastercycler ep gradient S [Eppendorf, Hauppauge, New York]). After this incubation, the Mastermix was added to the heated PCR tubes, and the tubes were placed back into the thermocycler. The program for the thermocycler was as follows: 95°C for 45 sec, 54-56°C for 45 sec, 72°C for 60 sec, repeat for 40 cycles (Table 2).

Following the PCR reactions for each hydrolase, agarose gel electrophoresis was performed to detect any PCR product produced. A 2% gel was prepared for PpIAR31, PpIAR32, and PpIAR34. This was done by mixing 1 g of DNA Agar (Marine BioProducts Inc., Delta, British Columbia, Canada) in 50 ml of 1x TAE, and 5 μ l stock EtBr (Thermo Fisher Scientific Inc., Waltham, Massachusetts). A 1.5% gel (0.75 g of DNA Agar in 50 ml of 1x TAE, and 5 μ l stock EtBr) was prepared for PpIAR33 and a second experiment with PpIAR31. The gels were electrophoresed in 1x TAE for 30 min

and then analyzed using an Ultra-Lum Electronic U.V. Transilluminator (Ultra-Lum Inc., Paramount, California).

Isolation and ligation of moss hydrolases into vectors

NeoScientific Labs (Cambridge, Massachusetts) constructed two pUC57 plasmids containing the PpIAR32 and PpIAR34 sequence inserts (Fig. 3a-b). Each of these two sequences was ligated into the plasmid at the BamHI site, but only the plasmid with the PpIAR34 insert contained a T7 promoter. We were given 4 µg of each plasmid, and diluted them to 100 ng/µl.

For re-cloning purposes into an expression vector, the PpIAR32 plasmid underwent PCR of the hydrolase insert. The primers employed to amplify the PpIAR32 insert were: forward primer 5'-GTTTCATGCAAGCATTGGTTT-3' and reverse primer 5'-GATCCCTGACCCATTTTTC-3'. The primers were obtained from Invitrogen (a division of Thermo Fisher Scientific Inc., Waltham, Massachusetts). The PCR reaction was set up with 2 µl of DNA, 1 µl of each primer, 12.5 µl of Mastermix (Denville Scientific Inc., Holliston, Massachusetts), and 8.5 µl of sterile DI water—equaling a total volume of 25 µl. A tube was set up with these contents and then placed into the thermocycler. The program for the thermocycler was as follows: 95°C for 45 sec, 56°C for 45 sec, 72°C for 60 sec, repeat for 35-40 cycles.

Following PCR, the PpIAR32 insert was “cleaned up” for ligation using materials repurposed from the QIAprep Spin Miniprep Kit, and the QIAGEN DNeasy Plant Mini Kit. The amount of QIAGEN “AP3” buffer and ethanol (1x) needed were determined by the volume of the insert (1x). The mixture was transferred into the QIAprep column. We

then centrifuged the column for 60 sec at 8,000 rpm. After centrifugation, we discarded the flow-through and added 500 μ l of the “AW” wash buffer (300 μ l “AW” stock buffer, 700 μ l EtOH) to the column. The column was again centrifuged for 60 sec at 8,000 rpm, and the flow-through was discarded. Another 500 μ l aliquot of the “AW” wash buffer was added to the column, and centrifugation followed for 2 min at 13,400 rpm. The flow-through was discarded and centrifugation was repeated with the same conditions (2 min, 13,400 rpm). Next, the column was transferred to a 1.5 ml microfuge tube and 40 μ l of 65°C sterile DI water was added to the column. This was incubated for 5 min at room temperature, before a final centrifugation for 1 min at 8,000 rpm. The concentration of the DNA was determined using a NanoDrop ND-1000 Spectrophotometer.

The purified DNA flow-through was used for blunt-end ligation. The PpIAR32 sequence insert was ligated in frame into a pETBlue-2 expression vector containing a promoter region (Fig. 3a) (Novagen, a brand of MilliporeSigma, Burlington, Massachusetts). We mixed 2 μ l of the insert (206 ng), 3 μ l of sterile water, and 5 μ l of “end conversion mix” (Novagen, a brand of MilliporeSigma, Burlington, Massachusetts; Novagen proprietary formula) equaling a total volume of 10 μ l. The purpose of the “end conversion mix” is to cleave off the extra bases and create blunt ends upon incubation. This mix was incubated at 26°C for 15 min, 75°C for 5 min, and on ice for 5 min. Following this incubation, centrifugation was employed to ensure mixing. Next, 1 μ l of the blunted pETBlue-2 vector and 1 μ l of DNA ligase were added. The complete mixture was then incubated overnight at 26°C.

Cloning and transformation of constructs

In order to transform the plasmids into bacterial cells, we performed heat shock transformation (Sambrook et al. 1989) with the PpIAR32 and PpIAR34 inserts into NovaBlue *E. coli* cells (Novagen, a brand of MilliporeSigma, Burlington, Massachusetts). Frozen competent NovaBlue *E. coli* cells were melted on ice for 5 min. We added between 1-5 μ l of the pETBlue-2 plasmid containing the PpIAR32 insert and the pUC57 plasmid containing the PpIAR34 insert and incubated this on ice for 5 min. We continued the incubation at 42°C for 45 sec, and then back on ice for 2 min. We sterilely added 250 μ l of Super Optimal Broth with Catabolite repression (SOC media) (Hanahan 1983) to the tube of cells and plasmid. This mixture was then incubated for 30 min at 37°C, before finally being spread onto LB plates that contained 50 μ g/ml of ampicillin as well as IPTG and X-gal for blue/white colony selection (imMedia Growth Medium, Thermo Fisher Scientific Inc., Waltham, Massachusetts). Blue colonies indicated that the insertion was not present in the vector, whereas white colonies indicated that ligation took place (Sambrook et al. 1989). Three LB/amp plates were set up as follows: two plates with 30 μ l of cells and 30 μ l of SOC media, and one plate with 240 μ l of cells. All three plates were then incubated for 24 h at 37°C. Following this incubation, sub-culturing was performed by selecting six white colonies from the PpIAR32 transformation plates, and six white colonies from the PpIAR34 transformation plates. Each colony was re-streaked onto a new LB/amp plate, as well as into a tube with 10 ml of liquid LB and 10 μ l of stock ampicillin (50 mg/ml). The LB/amp plates were incubated for 24 h at 37°C, and the tubes were incubated for 24 h on a shaker at 37°C and 250 rpm.

Synbio Technologies (Monmouth Junction, New Jersey) synthesized a pUC57 plasmid for us that contained the MpILR1 sequence insert at the BamHI site along with a T7 promoter for expression (Fig. 3c). For this reason, we were able to directly transform this construct into NovaBlue *E. coli* cells using the same protocol described above. Two additional liverwort expression constructs were made for us by Synbio Technologies— Δ MpILR1 and L244S-MpILR1 (Fig. 3c). Both of these liverwort sequences were also inserted into pUC57 plasmids at the BamHI site and contained T7 promoter regions. Again, we directly transformed these sequences into NovaBlue *E. coli* cells.

Plasmid DNA extraction

Plasmid DNA was extracted from PpIAR32, PpIAR34, MpILR1, Δ MpILR1 and L244S-MpILR1 using the QIAprep Spin Miniprep Kit (QIAGEN, Hilden, Germany). The miniprep was performed using the liquid cultures of cells after 24 h of incubation on the shaker. We centrifuged 2 ml of cells for 1 min at 13,400 rpm, and disposed of the supernatant. We then resuspended the pellet in 250 μ l of QIAGEN “P1” buffer (50 mM Tris•Cl [pH 8.0], 10 mM EDTA) and 1 μ l of RNase. After inverting the tube several times to mix the contents, we added 250 μ l of “P2” buffer (200 mM NaOH, 1% SDS [w/v]) and again inverted the tube several times. We repeated this same process by adding 350 μ l of “N3” buffer (QIAGEN proprietary formula) and inverted the tube several times to mix together the contents. The mixture was then centrifuged for 10 min at 13,400 rpm. Next, we decanted the supernatant into the QIAprep column. We centrifuged the column for 1 min at 13,400 rpm, and discarded the flow-through. This was followed by adding 750 μ l of “PE” buffer (200 μ l “PE” stock buffer [QIAGEN

proprietary formula], 800 μ l EtOH) to the column, and centrifuging it for 1 min at 13,400 rpm. The flow-through from the column was discarded, and another centrifugation was done for 1 min at 13,400 rpm to remove any remaining buffer. At this point, we removed the column and placed it into a sterile 1.5 ml microfuge tube. We added 50 μ l of room temperature sterile water to the column, incubated it at room temperature for 1 min, centrifuged it at 13,400 rpm for 1 min, disposed of the column, and stored the DNA flow-through at -20°C . We performed UV Spectrophotometry using a NanoDrop ND-1000 Spectrophotometer to check the DNA concentration of our plasmids.

Digests and sequencing

Endonuclease digests were performed with all samples to ensure correct construction of our hydrolase inserts. Eight reaction tubes were set up for the Δ MpILR1 endonuclease digest. Each of the tubes contained 1.5-2 μ l of purified plasmid DNA, 14-14.5 μ l of sterile DI water, 1 μ l of BSA [10mg/ml] (New England BioLabs, Ipswich, Massachusetts), 2 μ l of “buffer 2” (NEBuffer 2 [NEB proprietary formula]; New England BioLabs, Ipswich, Massachusetts), and 1 μ l of the BamHI enzyme (New England BioLabs, Ipswich, Massachusetts)—equaling a total volume of 20 μ l. The tubes were incubated for 2 h at 37°C in the thermocycler. Following removal from the thermocycler, gel electrophoresis was performed. A 0.7% gel was prepared by mixing 0.35 g of DNA Agar in 50 ml of 1xTAE and 5 μ l of stock EtBr. The 1x TAE gels were electrophoresed for 30 min and then analyzed using an Ultra-Lum Electronic U.V. Transilluminator. The endonuclease digests for PpIAR32, PpIAR34, MpILR1, and L244S-MpILR1 were prepared and run using similar protocols (Table 3).

Sequencing was performed with all samples to ensure correct construction of our hydrolase inserts. The protocols of Applied Biosystems (a division of Thermo Fisher Scientific Inc., Waltham, Massachusetts) were followed, which utilize the BigDye Terminator v3.1 Cycle Sequencing Kit (Thermo Fisher Scientific Inc., Waltham, Massachusetts). The samples underwent sequencing using an Applied Biosystems 3130 Genetic Analyzer.

Expression induction and protein extraction

In order to extract the expressed proteins from the PpIAR32, PpIAR34, MpILR1, Δ MpILR1 and L244S-MpILR1 plasmids, we set up liquid cultures for each plasmid in 15 ml of liquid LB and 15 μ l of stock ampicillin (50 mg/ml), to get a total concentration of 50 μ g/ml of ampicillin. We then placed the culture on a shaker at 37°C and 250 rpm to incubate overnight. The next morning another culture was started that contained 100 ml of liquid LB, 100 μ l of stock ampicillin, and 10 ml of the overnight liquid culture. This culture was left to incubate on the shaker for 2 h at 250 rpm and 37°C. After 2 h, 500 μ l of 1M IPTG was added to the liquid culture, and was again left to incubate on the shaker for 4 h at 250 rpm and 37°C. Upon removing the culture from the shaker, we transferred the liquid culture into nylon centrifuge tubes, and centrifuged 5 min at 6,000 rpm at 10°C. The supernatant was disposed of, and the pellet was resuspended in 1 ml of lysozyme buffer (30 mM Tris-HCl, pH 8.0, 1 mM EDTA, 20% sucrose, 1 mg/ml lysozyme), 1 ml of glycerol, 5 μ l of DNase, and 5 μ l of RNase (Campanella et al. 2003b). This mixture was sonicated on ice using a Microson Ultrasonic Cell Disruptor (Misonix Inc., Farmingdale, New York) at full power for 1 min, followed by a 1 min cool down.

This process was repeated three times, and 200 μ l aliquots of the protein extract were placed into 0.5 ml microfuge tubes and stored at -80°C .

Hydrolase assays

Hydrolase assays were prepared by using the frozen protein extract, assay buffer (100 mM Tris, pH 8.0, 10 mM MgCl_2 , 100 μ M MnCl_2 , 50 mM KCl, 100 μ M PMSF, 1 mM DTT, 10% sucrose), and various auxin amino acid conjugates (Ludwig-Müller et al. 1996; Campanella et al. 2003b). The auxin amino acid conjugates used were IAA-Alanine, IAA-Glycine, IAA-Aspartate, IAA-Leucine, IAA-Isoleucine, IAA-Valine, IAA-Phenylalanine, IPA-Alanine, and IBA-Alanine. All amino acid conjugates were obtained from Sigma-Aldrich (a brand of MilliporeSigma, Burlington, Massachusetts), with the exception of IPA-Alanine which was made in our laboratory (Campanella et al. 2004). The components of the assay were determined based on the concentration of the stock auxin amino acid conjugate. The IAA-Alanine, IAA-Glycine, IAA-Aspartate, IAA-Isoleucine, and IAA-Phenylalanine conjugates had a stock concentration of 10 mM. Therefore, the assays were prepared with 200 μ l of the protein extract, 290 μ l of the assay buffer, and 10 μ l of the auxin amino acid conjugate. Likewise, the IAA-Leucine, IAA-Valine, and IPA-Alanine conjugates had a stock concentration of 5 mM. Therefore, the assays were prepared with 200 μ l of the protein extract, 280 μ l of the assay buffer, and 20 μ l of the auxin amino acid conjugate. Lastly, the IBA-Alanine conjugate had a stock concentration of 6.66 mM.

The assay was prepared with 200 μ l of the protein extract, 285 μ l of the assay buffer, and 15 μ l of the auxin amino acid conjugate. After preparing these enzyme assays,

they were incubated at 40°C for 1 h. After incubation, we added 100 µl of 1M HCl to halt hydrolysis and 600 µl of ethyl acetate to the mixture and incubated this at room temperature for 5 min. This was followed by a 1 min centrifugation at 13,400 rpm. We then transferred the upper organic phase to a new microfuge tube and evaporated it using the SpeedVac (Savant SpeedVac SC110, Savant Refrigerated Condensation Trap RT100, Savant Two Stage VP190, Thermo Fisher Scientific Inc., Waltham, Massachusetts) on a medium setting for 20 min. The evaporated pellet was then resuspended with 200 µl of the appropriate running buffer. The IAA-Alanine, IAA-Glycine, IAA-Aspartate, IPA-Alanine, and IBA-Alanine conjugates were resuspended in 50% methanol; the IAA-Leucine, IAA-Isoleucine, IAA-Valine, and IAA-Phenylalanine conjugates were resuspended in 50% methanol/1% acetic acid. The pellet was resuspended to ensure complete mixture with the running buffer. This was then incubated an additional 5 min at 40°C in order to dissolve the pellet. We then centrifuged the mixture for 1 min at 13,400 rpm. Simultaneously, we prepared the high pressure liquid chromatography (Waters 510 HPLC Pump [Waters Corporation, Milford, Massachusetts]; LDC Analytical spectroMonitor 3200 variable wavelength detector [Laboratory Data Control, a division of Milton Roy Co., Riviera Beach, Florida]; Phenomenex C18 column [Phenomenex Inc., Torrance, California]) system for injection of these samples. The HPLC system was washed with 100% methanol at a rate of 2 ml/min for 10 min, and then at a rate of 1 ml/min for 10 min. This was followed by washing the machine with the appropriate running buffer (50% methanol or 50% methanol with 1% acetic acid) at a rate of 2 ml/min for 10 min.

After the system was equilibrated, we reduced the rate of the running buffer to 1 ml/min, and injected our sample into the HPLC system. This hydrolysis assay was repeated about 3-6 times for each auxin amino acid conjugate, with each of the protein extracts—PpIAR32, PpIAR34, MpILR1, Δ MpILR1 and L244S-MpILR1. The HPLC data was collected and analyzed using the WinDaq Data Acquisition Software (DATAQ, Akron, Ohio). The only noteworthy change was the replacement of our column with a Thermo Scientific C18 column (Thermo Fisher Scientific Inc., Waltham, Massachusetts) during our analysis of the L244S-MpILR1 liverwort construct. It was necessary for us to replace the column due to the inability of the HPLC system to complete the equilibration washing.

All background controls were performed using untransformed NovaBlue *E. coli* cells. Liquid cultures were set up with these cells similarly to the protein extraction protocol as described previously. These cultures, however, were not induced. These cells then underwent the same hydrolase assay protocol as described above.

Codon usage analysis

Principal coordinate analysis based on codon usage was performed using the PpIAR3 hydrolase family within archaea, eubacteria, bryophytes, gymnosperms, monocots, and dicots. CUSP (a program within the European Molecular Biology Open Source Software [EMBOSS] suite) was used to obtain the relative abundance values (J. V. Smalley, unpublished method, 2016). These values were then input into *vegan* (Oksanen et al. 2016) to obtain a dissimilarity matrix (Bray and Curtis 1957). The data from the dissimilarity matrix was used to perform the principal coordinate analysis via

classical multidimensional scaling (R Core Team, 2014; Gower 2015). The two-dimensional plots were created using *ggplot2* (Wickham 2009), and the three-dimensional plots were created using CAR (Companion to Applied Regression) (Fox and Weisburg 2011). All programs were used with default settings.

Phylogenetic tree construction

Alignments of all hydrolase homologs were created with the CLUSTAL X software, using its default configurations (Thompson et al. 1997). The data obtained from the CLUSTAL X analysis was used to create phylogenetic trees via the neighbor-joining method set to perform 1000 bootstraps (Saitou and Nei 1987; Felsenstein 1985), and then visualized using TreeView (Page 1996).

Results

Moss Results

Initial identification and phylogenetics

A BLAST search of the *P. patens* genome using the AtIAR3 homolog as a search probe yielded four hydrolase homologs—PpIAR31, PpIAR32, PpIAR33, and PpIAR34 (Table 1) (Skibitski 2016). We generated an amino acid similarity matrix to determine the structural resemblance of our moss hydrolases with other hydrolase homologs (Table 4). Only PpIAR32, -33, and -34 were included within the amino acid similarity matrix; PpIAR31 was purposefully omitted because it was determined later that the hydrolase is not a part of the *P. patens* genome. Overall, the moss hydrolases show only a moderate degree of amino acid similarity to hydrolases from other species. Based upon averages, the moss hydrolases are 50.5% similar to a previously identified cyanobacteria hydrolase, 43.4% similar to an algal hydrolase, 41.3% similar to a liverwort hydrolase (MpILR1), 45.5% similar to fern hydrolases, 41.0% similar to gymnosperm hydrolases, and 44.2% similar to angiosperm hydrolases.

A phylogenetic tree was constructed by Skibitski (2016), that focuses on the relationships between the moss hydrolases and other previously identified hydrolases originating from gymnosperm and angiosperm species (Fig. 4a). Based on 1000 bootstrap replicates, there is a high probability of accuracy for this phylogenetic tree. The tree shows clear divergences between moss, gymnosperms, and angiosperms—all of which have a >90% probability of accuracy. The inclusion of the bacterial species *Campylobacter jejuni* was used as an outgroup control species.

Codon usage analysis

Previous analyses of hydrolase genes employing the BASFv1.1 genome have exhibited soil bacteria genomic contamination (personal communication J. Ludwig-Müller). In an effort to investigate the integrity of our newly identified moss hydrolases, principal coordinate analysis based on codon usage of the PpIAR3 hydrolase family was analyzed within various archaea, eubacteria, bryophytes, gymnosperms, monocots, and dicot species (Fig. 5a, b). The purpose of this data was to analyze the phylogenetic relationships among different plant groups, in relation to hydrolase genes. We found that the hydrolase genes originating from monocots and dicot species fully intersect with the genes from gymnosperm species—the group from which they share most recent common ancestry. Tracing back evolutionarily, we next examined the bryophyte hydrolase genes. We found that the genes originating from the bryophytes intersect with the eubacteria and archaea genes, rather than any other plant genes.

Genomic DNA extraction from moss and PCR analysis

Upon performing the principal coordinate analysis and discovering that our moss hydrolases more closely resemble eubacteria and archaea rather than any other plant genes, we were again concerned about the prospect of bacterial genomic contamination. In an effort to further investigate whether the moss hydrolases PpIAR31-34 are endogenous to the *P. patens* genome or contamination, genomic DNA was extracted from a sample of dried moss tissue, PCR amplified using specific primers for each hydrolase gene, and analyzed for amplification through gel electrophoresis. The gel analysis of PpIAR31 only shows bands from the 18S positive control samples (Fig. 6a). Had the

experimental samples appeared on the gel, PpIAR31 fragments would have been apparent at 364 bp. The absence of the experimental samples on the gel indicates that the moss hydrolase PpIAR31 is not part of the *P. patens* genome. On the other hand, the gel analyses of PpIAR32, -33, and -34 all show fragments from the experimental and positive control samples (Fig. 6b-d). The bands from PpIAR32 were 256 bp in length, from PpIAR33 were 290 bp, and from PpIAR34 were 257 bp. In each case, the control samples which utilized the universal 18S primers can be seen at 324 bp. The presence of the experimental samples on the gels for PpIAR32, -33, and -34 indicate that these hydrolase genes are part of the *P. patens* genome.

Endonuclease digests

To ensure correct construction our PpIAR32 and PpIAR34 hydrolase inserts, endonuclease digests were performed and analyzed using gel electrophoresis (Fig. 7). Complete and correct digestion yields two bands—one representing the length of the insert, and another representing the remaining length of the plasmid. Specifically, correct digestion of the PpIAR32 insert should have yielded bands at 1172 bp and 3657 bp, based upon cutting sites employed by the SacI restriction enzyme (Fig. 7a). Lane 6, representing DNA sample #5, yielded complete digestion. Because the PpIAR34 insert was constructed within a pUC57 plasmid containing a T7 promoter, digestion was not needed to determine whether or not the insert was present. Rather, we linearized the plasmid to ensure that it was the correct size to account for the plasmid containing the insert. Correct digestion of the PpIAR34 containing plasmid should have yielded a band at 4100 bp, based upon the cutting site employed by the EcoRV restriction enzyme (Fig.

7b). Lanes 2-4, representing all three DNA samples, were all linearized and yielded a band at 4100 bp. Following successful digestion of our two moss inserts, we were able to proceed with our experiments to characterize each of the hydrolases.

Hydrolase assays

Hydrolase assays were prepared using protein extract from PpIAR32 and PpIAR34 to evaluate enzymatic activity and substrate specificity of various amino acid auxin conjugates. High pressure liquid chromatography (HPLC) was used to detect and measure levels of conjugate hydrolysis among the moss hydrolase genes. When performing HPLC, peaks were detected representing the nucleic acid, hydrolyzed auxin, and amino acid auxin conjugate (Fig. 8). We were able to locate the hydrolysis peak by comparison with the retention times of standard controls of auxin and the specific amino acid auxin conjugate being tested. Standard curves were generated for each auxin using different concentrations of the given auxin and were used to measure the volume under the hydrolysis peak. The volume under the hydrolysis peak represents the amount of auxin hydrolyzed over a period of 60 mins. Values were divided by 60 to obtain the amount of auxin hydrolyzed per min.

The PpIAR32 hydrolase showed no level of enzymatic activity across any of the amino acid auxin conjugates tested (Table 5). On the other hand, PpIAR34 demonstrated relatively high levels of enzymatic activity across the majority of amino acid auxin conjugates tested (Table 5). The PpIAR34 hydrolase was able to hydrolyze IAA-Alanine, IAA-Leucine, IAA-Isoleucine, IAA-Phenylalanine, and IBA-Alanine. The IBA-Alanine had the best substrate recognition and highest level of hydrolysis among all of the amino

acid auxin conjugates tested. On the other hand, the PpIAR34 hydrolase showed no level of enzymatic activity with the IAA-Glycine, IAA-Aspartate, and IPA-Alanine.

Liverwort Results

Initial identification and phylogenetics

A BLAST search of the *M. polymorpha* genome using the PsIAR3 homolog (Campanella et al. 2011) as a search probe yielded one hydrolase homolog—MpILR1 (Table 1). The liverwort hydrolase was named “MpILR1” after an NCBI protein BLAST search showed that the sequence was more similar to the ILR hydrolases than IAR hydrolases; specifically, MpILR1 has a 63.3% amino acid homology to *Arabidopsis thaliana* ILR.

In an effort to investigate the similarity of MpILR1 to other hydrolase homologs, an amino acid similarity matrix was created (Table 4). Overall, MpILR1 shows a high degree of amino acid similarity to other hydrolases. The liverwort hydrolase is 47.6% similar to a previously identified cyanobacteria hydrolase and 59.5% similar to an algal hydrolase. Based on averages, the liverwort hydrolase is 41.3% similar to previously identified moss hydrolases (PpIAR32-34), 60.2% similar to fern hydrolases, 59.6% similar to gymnosperm hydrolases, and 61.8% similar to angiosperm hydrolases.

Another phylogenetic tree was constructed that focuses on the relationships between the liverwort hydrolase and other previously identified algal and tracheophyte hydrolases (Fig. 4b). Based on 1000 bootstrap replicates, the liverwort hydrolase was placed in between the algal and fern hydrolases. The tree shows clear divergences

between early land plants, gymnosperms, and angiosperms—most of which have a $\geq 50\%$ probability of accuracy.

MpILR1's structure is novel in that it contains a stretch of an extra 11 amino acids compared to all other previously identified hydrolases. The nucleotide sequence—GGCACCTCATTCCTGTAAAGTCTCGAACATTAC—spans from position 834-866. The structure of MpILR1 is also noteworthy because it contains a Cysteine at amino acid position 137, a Glutamic Acid at amino acid position 173, and Histidine at positions 139, 197, and 397. The presence of these five amino acids is important because they lie within the active site of our hydrolase—an M20 metallopeptidase (Rawlings and Barrett, 1993; Bitto et al. 2009). Metallopeptidases rely on a co-factor to initiate enzymatic activity, and it is characteristic of M20 metallopeptidases to utilize zinc (Rawlings and Barrett, 1993). However, our hydrolase belongs to the M20D peptidase family, which has altered active sites that bind manganese as their co-factor rather than zinc (Bitto et al. 2009). It has been determined that the five amino acids—Cys137, Glu173, His139, His197, and His397—are likely involved in the binding of manganese in M20D metallopeptidases (Bitto et al. 2009). In our own analysis, we have observed this conserved domain in our liverwort hydrolase, as well as gymnosperm and angiosperm hydrolases (Fig. 9).

Copy number genetic redundancy occurs when two or more genes encode for the same biological function. We have observed this phenomenon during our analysis of bryophyte hydrolases from *P. patens* and *M. polymorpha*. Upon comparison of our hydrolases (PpIAR31, -32, -33, -34, and MpILR1) with previously identified tracheophyte hydrolases, we have observed a clear increase in the overall copy number of hydrolases within plant species (Table 6). Liverwort is the oldest extant land plant, and

we have only been able to identify one liverwort hydrolase gene from *M. polymorpha*. Moss species evolved later, and we were able to identify four hydrolase genes within *P. patens*. Gymnosperm evolution followed the bryophytes, and we have identified four hydrolases in both *Picea sitchensis* and *Pinus taeda*. The occurrence of copy number genetic redundancy becomes even more apparent in the angiosperm species. In monocot species, up to 11 copies of hydrolase genes have been observed (*Zea mays*), and in dicot species, up to 15 copies of hydrolase genes have been observed (*Vitis vinifera*). From an evolutionary standpoint, as later species evolved, more copies of hydrolase genes have been observed in plant genomes.

Codon Usage Analysis

The initial principal coordinate analysis based on codon usage that we performed uncovered that our moss hydrolases more closely resemble eubacteria and archaea rather than plant genes. Further investigation led us to discover that PpIAR31 is not a part of the *P. patens* genome. Given this finding, we were again concerned about the prospect of bacterial genomic contamination with our liverwort hydrolase. Therefore, principal coordinate analysis based on codon usage was repeated, taking into account our newly identified liverwort hydrolase (Fig. 5c). Various species of archaea, eubacteria, and eukaryotes (plants and algae) were analyzed to evaluate the phylogenetic relationships among different plant groups, in relation to hydrolase genes. We found that our liverwort hydrolase falls in line with hydrolases from other eukaryotes, rather than hydrolases from eubacteria and archaea. MpILR1 exhibited both protein and DNA homology with other plant hydrolases.

Endonuclease digests

To ensure correct construction our MpILR1, Δ MpILR1, and L244S-MpILR1 hydrolase inserts, endonuclease digests were performed and analyzed using gel electrophoresis (Fig. 7). Complete and correct digestion yields two bands—one representing the length of the insert, and another representing the remaining length of the pUC57 plasmid. Specifically, correct digestion of the MpILR1 insert should have yielded bands at 1756 bp and 2710 bp, based upon cutting sites employed by the BamHI restriction enzyme (Fig. 7c). The two lowest bands represent the insert and remaining length of the plasmid—all other bands represent incomplete digestion. Correct digestion of the Δ MpILR1 insert should have yielded bands at 1735 bp and 2710 bp, also based upon cutting sites employed by BamHI (Fig. 7d). Lane 5, representing DNA sample #4, yielded complete digestion. Correct digestion of the L244S-MpILR1 insert should have yielded bands at 1756 bp and 2710 bp from the BamHI enzyme (Fig. 7e). A gel was run with 5 DNA samples, but none were completely digested. Since DNA samples #1 and #2 were the closest to complete digestion, they were re-digested. This time, lane 2 representing DNA sample #1 yielded complete digestion.

Hydrolase assays

Hydrolase assays were prepared using protein extract from MpILR1 to evaluate enzymatic activity and substrate specificity of various amino acid auxin conjugates. High pressure liquid chromatography (HPLC) was used to detect and measure levels of hydrolysis among the liverwort hydrolase genes, following the same criteria as the moss hydrolase assays (Fig. 8). The MpILR1 liverwort hydrolase was unable to hydrolyze most

amino acid auxin conjugates (Table 5). The only two substrates that were recognized and hydrolyzed at very low levels were IAA-Leucine and IPA-Alanine.

We created an altered construct of our liverwort hydrolase, in which the extra 11 amino acid sequence within the active site was deleted (Fig. 3c). We wanted to determine the significance of this extra sequence within the active site, and the potential role it plays in hydrolysis. We dubbed this construct Δ MpILR1, and followed the same criteria for detecting and measuring levels of hydrolysis. The mutated hydrolase resulted in a complete loss of enzymatic function. No level of enzymatic activity was recorded across any of the amino acid auxin conjugates tested (Table 5).

We synthesized a third construct of our liverwort hydrolase, in which the amino acid at position 244 within the active site was changed from a Leucine to a Serine (Fig. 3c). We created this construct in part because all tracheophyte hydrolases observed had a Serine at this position. The most convincing evidence for this alteration was provided by X-ray crystallography analyses (Bitto et al. 2009). Bitto et al. (2009) determined that a Serine to Leucine mutation within the active site of a hydrolase does affect the binding capacity of the hydrolase. Specifically, the Leucine is considered a “bulkier, hydrophobic residue”, and impacts binding capacity (Bitto et al. 2009). For this reason, we decided to “fix” the mutated Leucine back to a Serine, and dubbed the construct L244S-MpILR1. We wanted to determine the significance of this mutation within the active site, and the potential role it plays in hydrolysis. The same criteria were followed for detecting and measuring levels of hydrolysis.

The L244S-MpILR1 enzyme showed higher levels of substrate recognition and enzymatic activity than the wild type hydrolase (Table 5). Substrate recognition was

gained and hydrolysis occurred with the IAA-Isoleucine and IBA-Alanine conjugates. Substrate recognition remained the same as MpILR1 for IAA-Leucine and IPA-Alanine. However, hydrolysis occurred at a higher rate in the mutated hydrolase. For example, hydrolysis of the IPA-Alanine conjugate increased more than 11-fold in the L244S-MpILR1 construct.

Discussion

Moss Discussion

Phylogeny

Upon analyzing our amino acid similarity matrix, it was discovered that on average our moss hydrolases are more similar to cyanobacteria hydrolases (50.5%) than hydrolases from any plant group (43.0%) (Table 4). In other words, the structure of our moss hydrolases more closely resembles “contaminating” bacterial hydrolases than plant hydrolases. Similarly, the codon usage analysis showed that the genes originating from the bryophytes intersect with the eubacteria and archaea genes rather than any other plant genes. This means that our moss hydrolases more closely resemble eubacteria and archaea hydrolases in terms of codon conservation than they do plants (Fig. 5a). From these analyses, we can conclude that our moss hydrolases structurally resemble those of bacteria.

The moss genomic PCR analysis showed that PpIAR31 appears not to be a part of the *P. patens* genome, while PpIAR32, -33, and -34 are present there (Fig. 6). We have concluded that PpIAR31 is likely the result of soil bacteria genomic contamination. When isolating the DNA from a moss specimen, it can be difficult to fully separate the moss from the soil in which it lives. Therefore, it is reasonable to infer that the *P. patens* v3.3 genome exhibits soil bacteria contamination. This would explain why we were able to identify the PpIAR31 hydrolase gene during our BLAST search of the *P. patens* genome, yet unable to verify the presence of the gene in a DNA sample from moss tissue. This also explains why the hydrolase looks more like bacteria.

However, it is clear that PpIAR32, -33, and -34 are a part of the *P. patens* genome (Fig. 6b-d). Even though the sequences structurally resemble bacteria, at the same time the structure does show some relation to plant peptidases. The five conserved domains that are characteristic of an M20D metallopeptidase and responsible for manganese binding within the active site (Cys137, Glu173, His139, His197, and His397) have been identified in all three of our moss hydrolases (Rawlings and Barrett, 1993; Bitto et al. 2009).

In an effort to explain why these three moss hydrolases structurally resemble bacteria, yet are found within the moss genome and show structure relation to plants, we propose that at some point in time horizontal gene transfer (HGT) occurred. Experiments have been done to investigate horizontal gene transfer within *P. patens*. Yue et al. (2012) identified 57 gene families that show evidence of HGT, including genes involved in purine degradation, stress responses, carbohydrate metabolism, glycolysis, DNA replication, peptidase activity, and hydrolase activity. It is possible that we have uncovered further genes which could be added to this list. Horizontal gene transfer has also previously been discussed as an explanation for how the TAA and YUC proteins utilized in synthesizing IAA may have arisen in land plants (Yue et al. 2014). In response to this topic, Wang et al. (2014) has proposed that HGT events are usually very complex and involve multiple steps. Wang et al. (2014) proposed that those proteins may have arisen in land plants either via HGT from bacteria to plants, HGT from bacteria to plants followed by another HGT from plants to bacteria, or separate HGT events from bacteria to land plants and bacteria to algae. The specific mechanisms of HGT within moss have been investigated (Yue et al. 2012). Given that mosses were some of the first terrestrial

plants and are effective at taking up foreign DNA, it is not surprising that mosses picked up genes via HGT from the bacterial and fungal inhabitants around them as they adjusted to terrestrial environments (Yue et al. 2012). Yue et al. (2012) hypothesizes that HGT from bacteria to moss likely occurs at two entry points in order for the foreign genes to be efficiently obtained and integrated within the moss genome: spore germination/early gametophyte development and fertilization/early embryo development. It is possible for HGT to occur from bacteria to moss during gametophyte development from spores because the gametophytes come in direct contact with soil and soil bacteria (Yue et al. 2012). It is possible for HGT to occur during fertilization and early embryo development because mosses keep their archegonia open during fertilization, exposing the eggs to the environment and foreign DNA around them (Yue et al. 2012).

Yue et al. (2012) also mentions that the timing of HGT events can be somewhat uncovered, based upon whether the gene of interest is observed in green algae. If the gene of interest is observed in green algae, then HGT likely occurred before the origin of land plants, and if the gene is not present in algae, then HGT likely occurred during or after the transition to terrestrial plants (Yue et al. 2012). In our case, our gene of interest is not present in green algae. In our proposal of HGT of the hydrolase genes from bacteria to moss, we have also taken into account the complexity of the process. We do not have any evidence to support *specifically when* HGT may have occurred, or *how many* times it may have occurred. Nonetheless, we conclude that HGT from bacteria to moss does provide a suitable explanation for the presence of PpIAR32, -33, and -34 within the *P. patens* genome.

Enzymology

Ludwig-Müller et al. (2009) speculated that the moss species, *Physcomitrella patens*, is a “dead end” in terms of auxin conjugate hydrolysis. On the contrary, upon characterization of the enzymatic activity of the PpIAR32 and PpIAR34 moss hydrolases, we determined that PpIAR32 showed no level of enzymatic activity, but PpIAR34 demonstrated relatively high levels of enzymatic activity across the majority of amino acid auxin conjugates tested (Table 5). In an effort to explain this contrast in activity, we again turn to horizontal gene transfer. If these moss genes were truly derived from bacteria, then it is possible that they might not all be functional within moss. It is possible that PpIAR32 is unable to hydrolyze auxin conjugates within moss, but is a functional hydrolase against different substrates within bacteria. This also suggests that HGT of PpIAR32 may have occurred relatively recently, because it is still a part of the *P. patens* genome and has yet to be lost from the genome due to a lack of function. Mosses have approximately 90% of their total IAA composition stored as conjugates, and only about 10% of free active IAA (Sztein et al. 1999). Given that mosses can function with small amounts of free active IAA, this may explain why we have only been able to identify one functional hydrolase within *P. patens* so far.

It should be noted, however, that even though we have identified PpIAR34 as the only functional hydrolase within *P. patens*, we have not fully elucidated its purpose as an auxin metabolism regulator. It is possible that mosses do not rely on active hydrolase genes and can sustain their physiological processes through the low levels of free IAA found within the plant, as well as low levels of background hydrolyzed IAA. We propose future experiments that focus on identifying whether PpIAR34 is even needed by *P.*

patens at all. In particular, we are interested in performing a knockout of PpIAR34 and analyzing how the moss is able to maintain its physiological processes. Through this experiment, we may uncover the true function of PpIAR34 within *P. patens*, as well as further insight into the hydrolase's role in the evolution of auxin metabolism regulation. We also plan to isolate and enzymatically characterize PpIAR33 to determine the hydrolase's function within *P. patens*. At the completion of this analysis we will have characterized all four moss hydrolases from *P. patens*, and hope to uncover the true purpose of these genes as auxin metabolism regulators within moss.

Liverwort Discussion

Phylogeny

Analysis of our amino acid similarity matrix suggests that on average our liverwort hydrolase is structurally most similar to angiosperm hydrolases (61.8%) (Table 4). MpILR1 also shows important structural relation to plant peptidases because it contains all five of the conserved M20D metallopeptidase domains responsible for manganese binding within the active site (Cys137, Glu173, His139, His197, and His397) (Fig. 9) (Rawlings and Barrett, 1993; Bitto et al. 2009). The codon usage analysis further confirmed that our liverwort hydrolase more closely resembles plants than eubacteria or archaea, because MpILR1 exhibited moderate protein and DNA homology with other plant hydrolases (Fig. 5c).

Our phylogenetic tree shows the ancestral relationships between hydrolases from algae, liverwort, fern, gymnosperms, and angiosperms (Fig. 4b). We are confident in the placement and grouping of each clade because of the high bootstrap values obtained in

our phylogenetic tree. The placement and grouping of each clade conforms with our general understanding of the evolution of plant groups. The moss phylogenetic analysis shows the ancestral relationships between hydrolases from bacteria, moss, gymnosperms, and angiosperms (Fig. 4a). We are also confident in the placement and grouping of each of these clades because of the high bootstrap values obtained. The purpose of each of these trees is to show the ancestry of our newly identified bryophyte hydrolases and the tracheophyte hydrolases which evolved after them. However, the issues are that these phylogenetic trees do not include both bryophyte species which we have investigated and each tree shows a different outgroup (bacteria vs. algae).

In an effort to combine these two phylogenetic analyses and portray the ancestry of our newly characterized moss and liverwort auxin amidohydrolase genes, we have proposed our own cladogram (Fig. 10). This cladogram combines our general knowledge of the evolution of plant groups and our new knowledge of our hydrolases and horizontal gene transfer. Whereas our liverwort hydrolase shares ancestry with a green algal ancestor, we propose that the moss hydrolases do not. Instead, we propose that after mosses diverged, they acquired their hydrolase genes via HGT. This cladogram explains why we saw a high degree of similarity between the liverwort and tracheophyte hydrolases, because they all share hydrolase ancestry with the green algal ancestor. On the other hand, this cladogram explains why we saw a high degree of similarity between the moss and bacterial hydrolases, as opposed to moss and tracheophyte hydrolases, because they do not share hydrolase ancestry with the green algal ancestor. We are confident in our proposal of HGT of the moss hydrolase genes from bacteria to moss. We

are interested in pursuing this analysis, and anticipate future experiments that confirm our cladogram and proposed hydrolase ancestry.

Enzymology

Upon characterization of the enzymatic activity of the MpILR1 liverwort hydrolase, we determined that the protein was unable to hydrolyze most amino acid auxin conjugates tested (Table 5). In an effort to explain why the liverwort hydrolase might be classified as a “low-functioning hydrolase”, we propose the phenomenon of exaptation. Gould and Vrba (1982) first coined the term as features that “were not built by natural selection for their current role”. In other words, a particular feature that once served one function, has evolved to serve another function. Since we were unable to observe any significant levels of auxin hydrolysis, it is possible that MpILR1 served another purpose in *M. polymorpha* and was eventually exapted over evolutionary time to achieve its full regulatory significance in tracheophytes. We also believe that exaptation is a suitable explanation for our “low-functioning” liverwort hydrolase because this bryophyte does not utilize auxin the same way that vascular plants do. As a small, non-vascular plant it does not rely on processes such as flowering and fruit ripening that are regulated by auxin. Rather, we believe that the low levels of free IAA found within liverwort, as well as the very low levels of hydrolyzed IAA are sufficient to provide the plant with enough auxin to regulate the processes of the small plant. Further, we propose that auxin conjugate hydrolysis likely did not become an active regulatory process until tracheophytes evolved.

Upon characterization of the enzymatic activity of our altered liverwort hydrolases, Δ MpILR1 and L244S-MpILR1, we determined that Δ MpILR1 resulted in a complete loss of enzymatic function, but L244S-MpILR1 demonstrated higher levels of substrate recognition and enzymatic activity than the wild type hydrolase (Table 5). While it remains unclear exactly what the function of the extra 11 amino acid sequence located near the active site is, we have concluded that it is important because its removal eliminates what little hydrolysis was originally observed. We performed an analysis on the structure of MpILR1 using SWISS-MODEL (<https://swissmodel.expasy.org>) and UCSF Chimera (<https://www.cgl.ucsf.edu/chimera/>), in order to visualize the structure of the 11 extra amino acid sequence. It was determined that the sequence is located behind the active site (Fig. 11). This has led us to propose that the removal of the sequence may lead to a change in the shape of the active site, and therefore a change in substrate recognition and enzymatic activity. What continues to perplex us is why the loss of the sequence is so important here, since the sequence is altogether absent from other species' hydrolases. We are interested in pursuing this analysis, and anticipate future experiments that determine why the loss of the 11 amino acid sequence is vital for MpILR1's function, yet irrelevant to the function of other hydrolase genes.

Further, in an effort to uncover the evolutionary change between a hydrolase from *M. polymorpha* and tracheophyte hydrolases, we analyzed the enzymatic function of L244S-MpILR1. We have concluded that the amino acid change from Leucine to Serine at amino acid position 244 is one of the essential structural changes that led to modern tracheophyte hydrolases. It remains unclear how many other vital structural changes may

have occurred. Nonetheless, we are confident that we have uncovered one clue that bridges the evolutionary gap between bryophyte and tracheophyte hydrolases.

Bibliography

- Andreae, W. A. and N. E. Good. 1957. Studies on 3-indoleacetic acid metabolism. IV. Conjugation with aspartic acid and ammonia as processes in the metabolism of carboxylic acids. *Plant Physiology*. 32: 566-572.
- Bajguz, A. and A. Piotrowska. 2009. Conjugates of auxin and cytokinin. *Phytochemistry*. 70: 957-969.
- Bandurski, R. S., J. D. Cohen, J. P. Slovin and D. M. Reinecke. 1995. Auxin biosynthesis and metabolism. In: Davies, P. J. *Plant Hormones: Physiology, Biochemistry and Molecular Biology* 2nd edn. Kluwer Academic Publishers. Boston, Massachusetts.
- Bartel, B. and G. R. Fink. 1995. ILR1, an amidohydrolase that releases active indole-3-acetic acid from conjugates. *Science*. 268: 1745-1748.
- Bayer, M. H. 1969. Gas chromatographic analysis of acidic indole auxins in *Nicotiana*. *Plant Physiology*. 44: 267-271.
- Bitto, E., C. A. Bingman, L. Bittova, N. L. Houston, R. S. Boston, B. G. Fox and G. N. Phillips Jr. 2009. X-ray structure of ILL2, an auxin-conjugate amidohydrolase from *Arabidopsis thaliana*. *Proteins*. 74: 61-71.
- Blommaert, K. L. J. 1954. Growth- and inhibiting-substances in relation to the rest period of the potato tuber. *Nature*. 174: 970-972.
- Boysen-Jensen, P. 1913. Über die Leitung des phototropischen Reizes in der Avenakoleoptile. *Berichte der Deutschen Botanischen Gesellschaft*. 31: 559-566.
- Bray, J. R. and J. T. Curtis. 1957. An ordination of the upland forest of Southern Wisconsin. *Ecological Monographs*. 27: 325-349.
- Campanella, J. J., D. Larko and J. Smalley. 2003a. A molecular phylogenetic analysis of the ILR1-like family of IAA amidohydrolase genes. *Comparative and Functional Genomics*. 4: 584-600.
- Campanella, J. J., J. Ludwig-Müller, V. Bakllamaja, V. Sharma and A. Cartier. 2003b. ILR1 and sILR IAA amidohydrolase homologs differ in expression pattern and substrate specificity. *Plant Growth Regulation*. 41: 215-223.
- Campanella, J. J., A. F. Olajide, V. Magnus and J. Ludwig-Müller. 2004. A novel auxin conjugate hydrolase from wheat with substrate specificity for longer side-chain auxin amide conjugates. *Plant Physiology*. 135: 2230-2240.

- Campanella, J. J., R. S. Skibitski, D. Schiller and J. Ludwig-Müller. 2011. Gymnosperm auxin conjugate hydrolases from *Picea sitchensis* (Sitka Spruce) and their implications on higher plant evolution. *Proceedings of the Plant Growth Regulation Society of America*. 37: 127-136.
- Campanella, J. J., J. V. Smalley and M. E. Dempsey. 2014a. A phylogenetic examination of the primary anthocyanin production pathway of the Plantae. *Botanical Studies*. 55: 10.
- Campanella, J. J., S. M. Smith, D. Leibu, S. Wexler and J. Ludwig-Müller. 2008. The auxin conjugate hydrolase family of *Medicago truncatula* and their expression during the interaction with two symbionts. *Journal of Plant Growth Regulation*. 27: 26-38.
- Campanella, J. J., N. Zaben, D. Enriquez, J. V. Smalley and J. Ludwig-Müller. 2014b. An enzymatic analysis of Loblolly pine and Sitka spruce auxin conjugate hydrolases and evolutionary implications. *Acta Horticulturae: International Society for Horticultural Science*. 1042: 79-88.
- Chisnell, J. R. 1984. Myo-inositol esters of indole-3-acetic acid are endogenous components of *Zea mays* L. shoot tissue. *Plant Physiology*. 74: 278-283.
- Chou, J. C., W. W. Mulbry and J. D. Cohen. 1998. The gene for indole-3-acetyl-l-aspartic acid hydrolase from *Enterobacter agglomerans*: molecular cloning, nucleotide sequence, and expression in *Escherichia coli*. *Molecular and General Genetics*. 259: 172-178.
- Cohen, J. D. and R. S. Bandurski. 1982. Chemistry and physiology of the bound auxins. *Annual Review of Plant Physiology*. 33: 403-430.
- Cooke, T. J., D. B. Poli, A. E. Szein and J. D. Cohen. 2002. Evolutionary patterns in auxin action. *Plant Molecular Biology*. 49: 319-338.
- Darwin, C. R. 1880. *The Power of Movements in Plants*. John Murray. London.
- Davies, P. J. 1995. *Plant Hormones: Physiology, Biochemistry and Molecular Biology*. Kluwer Academic Publishers. Dordrecht, the Netherlands.
- Davies, R. T., D. H. Goetz, J. Lasswell, M. N. Anderson and B. Bartel. 1999. IAR3 encodes an auxin conjugate hydrolase from *Arabidopsis*. *The Plant Cell*. 11: 365-376.
- Felsenstein, J. 1985. Confidence limits on phylogenies: an approach using the bootstrap. *Evolution*. 39: 783-791.
- Feung, C. S., R. H. Hamilton and R. O. Mumma. 1976. Metabolism of indole-3-acetic acid III. Identification of metabolites isolated from crown gall callus tissue. *Plant Physiology*. 58: 666-669.

- Feung, C. S., R. H. Hamilton and R. O. Mumma. 1977. Metabolism of indole-3-acetic acid IV. Biological properties of amino acid conjugates. *Plant Physiology*. 59: 91-93.
- Fitting, H. 1907. Die Leitung Tropischer Reize in parallelotropen Pflanzenteilen. *Jahrbücher für wissenschaftliche Botanik*. 44: 177-253.
- Fox, J. and S. Weisberg. 2011. *An R Companion to Applied Regression* 2nd edn. SAGE Publications Inc. Thousand Oaks, California.
- Friml, J., A. Vienten, M. Sauer, D. Weijers, H. Schwarz, T. Hamann, R. Offringa and G. Jürgens. 2003. Efflux-dependent auxin gradients establish the apical-basal axis of *Arabidopsis*. *Nature*. 426: 147-153.
- Gould, S. J. and E. S. Vrba. 1982. Exaptation-A Missing Term in the Science of Form. *Paleobiology*. 8: 4-15.
- Gower, J. C. 2015. Principal Coordinates Analysis. *Wiley StatsRef: Statistics Reference Online*. 1-7.
- Graham, L. E. 1993. *Origin of land plants*. John Wiley & Sons. New York.
- Gray, J. 1993. Major Paleozoic land plant evolutionary bio-events. *Palaeogeography, Palaeoclimatology, Palaeoecology*. 104: 153-169.
- Haagen-Smit, A. J., W. B. Dandliker, S. H. Wittwer and A. E. Murneek. 1946. Isolation of 3-indoleacetic acid from immature corn kernels. *American Journal of Botany*. 33: 118-120.
- Hanahan, D. 1983. Studies on transformation of *Escherichia coli* with plasmids. *Journal of Molecular Biology*. 166: 557-580.
- Hori, K., F. Maruyama, T. Fujisawa, T. Togashi, N. Yamamoto, M. Seo, S. Sato, T. Yamada, H. Mori, N. Tajima, T. Moriyama, M. Ikeuchi, M. Watanabe, H. Wada, K. Kobayashi, M. Saito, T. Masuda, Y. Sasaki-Sekimoto, K. Mashiguchi, K. Awai, M. Shimojima, S. Masuda, M. Iwai, T. Nobusawa, T. Narise, S. Kondo, H. Saito, R. Sato, M. Murakawa, Y. Ihara, Y. Oshima-Yamada, K. Ohtaka, M. Satoh, K. Sonobe, M. Ishii, R. Ohtani, M. Kanamori-Sato, R. Honoki, D. Miyazaki, H. Mochizuki, J. Umetsu, K. Higashi, D. Shibata, Y. Kamiya, N. Sato, Y. Nakamura, S. Tabata, S. Ida, K. Kurokawa and H. Ohta. 2014. *Klebsormidium flaccidum* genome reveals primary factors for plant terrestrial adaptation. *Nature communications*. 5: 3978.
- Jirásková, D., A. Poulíčková, O. Novák, K. Sedláková, V. Hradecká and M. Strnad. 2009. High-throughput screening technology for monitoring phytohormones production in microalgae. *Journal of Phycology*. 45: 108-118.

- Junghans, U., A. Polle, P. DÜchting, E. Weiler, B. Kuhlmann, F. Gruber and T. Teichmann. 2006. Adaptation to high salinity in poplar involves changes in xylem anatomy and auxin physiology. *Plant Cell and Environment*. 29: 1519-1531.
- Kleczkowski, K. and J. Schell. 1995. Phytohormone conjugates: nature and function. *Critical Reviews in Plant Sciences*. 14: 283-298.
- Koepfli, J. B., K. V. Thimann and F. W. Went. 1938. Phytohormones: structure and physiological activity I. *Journal of Biological Chemistry*. 122: 763-780.
- Kögl, F. and A. J. Haagen-Smit. 1931. Über die Chemie des Wuchsstoffs. *Proceedings of the Koninklijke Nederlandse Akademie van Wetenschappen*. 34: 1411-1416.
- Kögl, F., H. Erxleben and A. J. Haagen-Smit. 1934a. Über die Isolierung der Auxine a und b aus pflanzlichen Materialien. IX. Mitteilung. *Hoppe-Seyler's Zeitschrift für Physiologische Chemie*. 243: 209-226.
- Kögl F., A. J. Haagen-Smit and H. Erxleben. 1934b. Über ein neues Auxin (Heteroauxin) aus Harn. XI. Mitteilung über pflanzliche Wachstumsstoffe. *Hoppe-Seyler's Zeitschrift für Physiologische Chemie*. 228: 90-103.
- Korasick, D. A., T. A. Enders and L. C. Strader. 2013. Auxin biosynthesis and storage forms. *Journal of Experimental Botany*. 64: 2541-2555.
- Kurdach, S., R. Skibitski, J. Mann, J. V. Smalley and J. J. Campanella. 2017. Characterizations of two auxin amidohydrolases from *Physcomitrella patens* and evidence for horizontal gene transfer from soil bacteria. Wehner Research Conference, Montclair State University. Poster.
- Lambrecht, M., Y. Okon, A. V. Broek and J. Vanderleyden. 2000. Indole-3-acetic acid: a reciprocal signaling molecule in bacteria-plant interactions. *Trends in Microbiology*. 8: 298-300.
- LeClere, S., R. Tellez, R. A. Rampey, S. P. T. Matsuda and B. Bartel. 2002. Characterization of a family of IAA-amino acid conjugate hydrolases from *Arabidopsis*. *Journal of Biological Chemistry*. 277: 20446-20452.
- Lee, S., M. Flores-Encarnación, M. Contreras-Zentella, L. Garcia-Flores, J. E. Escamilla and C. Kennedy. 2004. Indole-3-acetic acid biosynthesis is deficient in *Gluconacetobacter diazotrophicus* strains with mutations in cytochrome *c* biogenesis genes. *Journal of Bacteriology*. 186: 5384-5391.
- Leliaert, F., D. R. Smith, H. Moreau, M. D. Herron, H. Verbruggen, C. F. Delwiche and O. De Clerck. 2012. Phylogeny and molecular evolution of the green algae. *Critical Reviews in Plant Sciences*. 31: 1-46.

- Lewis, L. A. and R. M. McCourt. 2004. Green algae and the origin of land plants. *American Journal of Botany*. 91: 1535-1556.
- Linsler, H., H. Mayr and F. Maschek. 1954. Papierchromatographie von zellstreckend wirksamen indolkörpern aus *Brassica*—Arten. *Planta*. 44: 103-120.
- Ljung, K., A. K. Hull, M. Kowalczyk, A. Marchant, J. Celenza, J. D. Cohen and G. Sandberg. 2002. Biosynthesis, conjugation, catabolism and homeostasis of indole-3-acetic acid in *Arabidopsis thaliana*. *Plant Molecular Biology*. 49: 249-272.
- Ludwig-Müller, J. 2011. Auxin conjugates: their role for plant development and in the evolution of land plants. *Journal of Experimental Botany*. 62: 1757-1773.
- Ludwig-Müller, J., E. L. Decker and R. Reski. 2009. Dead end for auxin conjugates in *Physcomitrella*? *Plant Signalling and Behavior*. 4: 116-118.
- Ludwig-Müller, J., E. Epstein and W. Hilgenberg. 1996. Auxin-conjugate hydrolysis in Chinese cabbage: Characterization of an amidohydrolase and its role during infection with clubroot disease. *Physiologia Plantarum*. 97: 627-634.
- Maruyama, A., M. Maeda and U. Simidu. 1989. Microbial production of auxin indole-3-acetic acid in marine sediments. *Marine Ecology Progress Series*. 58: 69-75.
- Mashiguchi, K., K. Tanaka, T. Sakai, S. Sugawara, H. Kawaide, M. Natsume, A. Hanada, T. Yaeno, K. Shirasu, H. Yao, P. McSteen, Y. Zhao, K. Hayashi, Y. Kamiya and H. Kasahara. 2011. The main auxin biosynthesis pathway in *Arabidopsis*. *Proceedings of the National Academy of Sciences of the United States of America*. 108, 18512–18517.
- Mauseth, J. D. 1991. *Botany: An Introduction to Plant Biology*. Pg 348-415. W. B. Saunders. Philadelphia.
- Nicholls, P. B. 1967. The isolation of indole-3-acetyl-3-O-*myo*-inositol from *Zea mays*. *Planta*. 10: 2207-2209.
- Nonhebel, H. M., T. P. Cooney and R. Simpson. 1993. The route, control and compartmentation of auxin synthesis. *Australian Journal of Plant Physiology*. 20: 527-539.
- Normanly, J. and B. Bartel. 1999. Redundancy as a way of life – IAA metabolism. *Current Opinion in Plant Biology*. 2: 207-213.
- Normanly, J., J. P. Slovin and J. D. Cohen. 1995. Rethinking auxin biosynthesis and metabolism. *Plant Physiology*. 107: 323-329.

- Oksanen, J., F. G. Blanchet, M. Friendly, R. Kindt, P. Legendre, D. McGlinn, P. R. Minchin, R. B. O'Hara, G. L. Simpson, P. Solymos, M. Henry, H. Stevens, E. Szoecs and H. Wagner. 2016. *vegan: Community Ecology Package*. R package version 2.4-1.
- Östin, A., M. Kowalczyk, R. P. Bhalerao and G. Sandberg. 1998. Metabolism of indole-3-acetic acid in *Arabidopsis*. *Plant Physiology*. 118: 285-296.
- Ouyang, J., X. Shao and J. Li. 2000. Indole-3-glycerol phosphate, a branchpoint of indole-3-acetic acid biosynthesis from the tryptophan biosynthetic pathway in *Arabidopsis thaliana*. *The Plant Journal*. 24: 327-333.
- Paal, A. 1918. Über phototropische Reizleitung. *Jahrbücher für wissenschaftliche Botanik*. 58: 406-458.
- Page, R. D. 1996. TREEVIEW: an application to display phylogenetic trees on personal computers. *Computer Applications in the Biosciences*. 12: 357-358.
- Parnell, J. and S. Foster. 2012. Ordovician ash geochemistry and the establishment of land plants. *Geochemical Transactions*. 13: 7.
- Pollman, S., D. Neu and E. W. Weiler. 2003. Molecular cloning and characterization of an amidase from *Arabidopsis thaliana* capable of converting indole-3-acetamide into the plant growth hormone, indole-3-acetic acid. *Phytochemistry*. 62: 293-300.
- Rampey, R. A., S. LeClere, M. Kowalczyk, K. Ljung, G. Sandberg and B. Bartel. 2004. A family of auxin-conjugate hydrolases that contributes to free indole-3-acetic acid levels during *Arabidopsis* germination. *Plant Physiology*. 135: 978-988.
- Raven, P. H., R. F. Evert and S. E. Eichhorn. 1992. *Biology of Plants*. Pg 545-572. Worth Publishers. New York.
- Rawlings, N. D. and A. J. Barrett. 1993. Evolutionary families of peptidases. *The Journal of Biochemistry*. 290: 205-218.
- R Core Team. 2014. R: A language and environment for statistical computing. R Foundation for Statistical Computing. Vienna, Austria.
- Rensing, S. A., D. Lang, A. D. Zimmer, A. Terry, A. Salamov, H. Shapiro, T. Nishiyama, P. F. Perroud, E. A. Lindquist, Y. Kamisugi, T. Tanahashi, K. Sakakibara, T. Fujita, K. Oishi, T. Shin-I, Y. Kuroki, A. Toyoda, Y. Suzuki, S. Hashimoto, K. Yamaguchi, S. Sugano, Y. Kohara, A. Fujiyama, A. Anterola, S. Aoki, N. Ashton, W. B. Barbazuk, E. Barker, J. L. Bennetzen, R. Blankenship, S. H. Cho, S. K. Dutcher, M. Estelle, J. A. Fawcett, H. Gundlach, M. Prigge, B. Reiss, T. Renner, S. Rombauts, P. J. Rushton, A. Sanderfoot, G. Schween, S. H. Shiu, K. Stueber, F. L. Theodoulou, H. Tu, Y. Van de Peer, P. J. Verrier, E. Waters, A. Wood, L. Yang, D. Cove, A. C. Cuming, M. Hasebe, S.

- Lucas, B. D. Mishler, R. Reski, I. V. Grigoriev, R. S. Quatrano and J.L. Boore. 2008. The *Physcomitrella* Genome reveals evolutionary insights into the conquest of land by plants. *Science*. **319**, 64-69.
- Romano, C. P., M. B. Hein and H. J. Klee. 1991. Inactivation of auxin in tobacco transformed with the indoleacetic acid-lysine synthetase gene of *Pseudomonas savastanoi*. *Genes and Development*. 5: 438-446.
- Saitou, N. and M. Nei. 1987. The neighbor-joining method: a new method for reconstructing phylogenetic trees. *Molecular Biology and Evolution*. 4: 406-425.
- Salisbury, F. B. and C. W. Ross. 1992. *Plant Physiology*. Pg 357-407, 531-548. Wadsworth Publishing Company, Inc. Belmont, California.
- Salkowski, E. 1885. Ueber das verhalten der skatolcarbonsäure im organismus. *Zeitschrift für physiologische Chemie*. 9: 23-33.
- Sambrook, J., E. F. Fritsch and T. Maniatis. 1989. *Molecular cloning: a laboratory manual* 2nd ed. Cold Spring Harbor Laboratory Press. Cold Spring Harbor, New York.
- Sanchez Carranza, A. P., A. Singh, K. Steinberger, K. Panigrahi, K. Palme, A. Dovzhenko and C. Dal Bosco. 2016. Hydrolases of the ILR1-like family of *Arabidopsis thaliana* modulate auxin response by regulating auxin homeostasis in the endoplasmic reticulum. *Scientific Reports*. 6: 24212.
- Savić, B., S. Tomić, V. Magnus, K. Gruden, K. Barle, R. Grenković, J. Ludwig-Müller and B. Salopek-Sondi. 2009. Auxin amidohydrolases from *Brassica rapa* cleave the alanine conjugate of indolepropionic acid as a preferable substrate: a biochemical and modeling approach. *Plant and Cell Physiology*. 50: 1587-1599.
- Scott, A. C. and I. J. Glasspool. 2006. The diversification of Paleozoic fire systems and fluctuations in atmospheric oxygen concentration. *Proceedings of the National Academy of Sciences of the United States of America*. 103: 10861-10865.
- Skibitski, R. 2016. The isolation and characterization of PpIAR31, an auxin conjugate amidohydrolase in *Physcomitrella patens* and its implications. Thesis in partial fulfillment of master's degree. Montclair State University, Montclair, New Jersey.
- Slovin, J. P., R. S. Bandurski and J. D. Cohen. 1999. Auxin. In: *Biochemistry and molecular biology of plant hormones*. (Eds: P. J. J. Hooykaas, M. A. Hall and K. R. Libbenga) Elsevier. Amsterdam, the Netherlands.
- Soding, H. 1925. Zur kenntnis der wuchshormone in der haferkoleoptile. *Jahrbücher für wissenschaftliche Botanik*. 64: 587-603.

- Spaepen, S. and J. Vanderleyden. 2011. Auxin and plant-microbe interactions. *Cold Spring Harbor Perspectives in Biology*. 3: a001438.
- Spena, A., E. Prinsen, M. Fladung, S. C. Schulze and H. Van Onckelen. 1991. The indoleacetic acid-lysine synthetase gene of *Pseudomonas syringae* subsp. *savastanoi* induces developmental alterations in transgenic tobacco and potato plants. *Molecular and General Genetics*. 227: 205-212.
- Staswick, P. E. 2009. The tryptophan conjugates of jasmonic and indole-3-acetic acids are endogenous auxin inhibitors. *Plant Physiology*. 150: 1310-1321.
- Stepanova, A. N., J. Robertson-Hoyt, J. Yun, L. M. Benavente, D. Y. Xie, K. Dolezal, A. Schlereth, G. Jurgens and J. M. Alonso. 2008. TAA1-mediated auxin biosynthesis is essential for hormone crosstalk and plant development. *Cell*. 133: 177–191.
- Stepanova, A. N., J. Yun, L. M. Robles, O. Novak, W. He, H. Guo, K. Ljung and J. M. Alonso. 2011. The *Arabidopsis* YUCCA1 flavin monooxygenase functions in the indole-3-pyruvic acid branch of auxin biosynthesis. *Plant Cell*. 23: 3961–3973.
- Stirk, W. A., V. Ördög, O. Novák, J. Rolčik, M. Strnad, P. Bálint and J. van Staden. 2013. Auxin and cytokinin relationships in 24 microalgal strains. *Journal of Phycology*. 49: 459-467.
- Strother, P. K., S. Al-Hajri and A. Traverse. 1996. New evidence for land plants from the lower Middle Ordovician of Saudi Arabia. *Geology*. 24: 55-58.
- Sugawara, S., S. Hishiyama, Y. Jikumaru, A. Hanada, T. Nishimura, T. Koshiba, Y. Zhao, Y. Kamiya and H. Kasahara. 2009. Biochemical analyses of indole-3-acetaldoxime-dependent auxin biosynthesis in *Arabidopsis*. *Proceedings of the National Academy of Sciences of the United States of America*. 106: 5430-5435.
- Sztein, A. E., J. D. Cohen and T. J. Cooke. 2000. Evolutionary patterns in the auxin metabolism of green plants. *International Journal of Plant Sciences*. 161: 849-859.
- Sztein, A. E., J. D. Cohen, I. García de la Fuente and T. J. Cooke. 1999. Auxin metabolism in mosses and liverworts. *American Journal of Botany*. 86: 1544-1555.
- Tabone, D. 1958. Biosynthèse par *B. megatherium* de combinaisons de l'acide indol propionique avec certains acides aminés. *Bulletin De La Société De Chimie Biologique (Paris)*. 40: 965-969.
- Tabone, J. and D. Tabone. 1953. Bio-estérification du glucose. V. Bio-synthèse par *Bacillus megatherium* de l'ester β glucosidique de l'acide indolpropionique. *Comptes Rendus Hebdomadaires des Séances de l'Académie des Sciences*. 237: 943–944.

- Tao, Y., J. L. Ferrer, K. Ljung, F. Pojer, F. Hong, J. A. Long, L. Li, J. E. Moreno, M. E. Bowman, L. J. Ivans, Y. Cheng, J. Lim, Y. Zhao, C. L. Ballaré, G. Sandberg, J. P. Noel and J. Chory. 2008. Rapid synthesis of auxin via a new tryptophan-dependent pathway is required for shade avoidance in plants. *Cell*. 133: 164–176.
- Theissen, G., T. Muenster and K. Henschel. 2001. Why don't mosses flower? *New Phytologist*. 150: 1-5.
- Thimann, K. V. 1935. On the plant growth hormone produced by *Rhizopus sinicus*. *Journal of Biological Chemistry*. 109: 279–291.
- Thimann, K. V. and J. B. Koepfli. 1935. Identity of the growth-promoting and root-forming substances of plants. *Nature*. 135: 101.
- Thompson, J. D., T. J. Gibson, F. Plewniak, F. Jeanmougin and D. G. Higgins. 1997. The Clustal X windows interface: flexible strategies for multiple sequence alignment aided by quality analysis tools. *Nucleic Acids Research*. 24: 4872-4882.
- Timme, R. E., T. R. Bachvaroff and C. F. Delwiche. 2012. Broad phylogenetic sampling and the sister lineage of land plants. *PLOS One*. 7: e29696.
- Wang, C., Y. Liu, S. S. Li and G. Z. Han. 2014. Origin of plant auxin biosynthesis in charophyte algae. *Trends in Plant Science*. 19: 741-743.
- Wellman, C. H., P. L. Osterloff and U. Mohiuddin. 2003. Fragments of the earliest land plants. *Nature*. 425: 282-285.
- Went, F. W. 1926. On growth-accelerating substances in the coleoptile of *Avena sativa*. *Proceedings of the Koninklijke Nederlandse Akademie Van Wetenschappen*. 30: 10-19.
- Went, F. W. 1928. Wuchsstoff und Wachstum. *Recueil des Travaux Botaniques Néerlandais*. 25: 1-116.
- White, R. H. 1987. Indole-3-acetic acid and 2-(indol-3-ylmethyl)indol-3-yl acetic acid in the thermophilic archaebacterium *Sulfolobus acidocaldarius*. *Journal of Bacteriology*. 169: 5859-5860.
- Wickham, H. 2009. *ggplot2: Elegant Graphics for Data Analysis*. Springer Publishing Company. New York, New York.
- Woodward, A. W. and B. Bartel. 2005. Auxin: regulation, action, and interaction. *Annals of Botany*. 95: 707-735.
- Won, C., X. Shen, K. Mashiguchi, Z. Zheng, X. Dai, Y. Cheng, H. Kasahara, Y. Kamiya, J. Chory and Y. Zhao. 2011. Conversion of tryptophan to indole-3-acetic acid by

TRYPTOPHAN AMINOTRANSFERASES OF ARABIDOPSIS and YUCCAs in *Arabidopsis*. *Proceedings of the National Academy of Sciences of the United States of America*. 108: 18518–18523.

Yue, J., X. Hu and J. Huang. 2014. Origin of plant auxin biosynthesis. *Trends in Plant Science*. 19: 764-770.

Yue, J., X. Hu, H. Sun, Y. Yang and J. Huang. 2012. Widespread impact of horizontal gene transfer on plant colonization of land. *Nature Communications*. 3: 1152.

Zenk, M. H. 1961. I-(indole-3-acetyl)- β -D-glucose, a new compound in the metabolism of indole-3-acetic acid in plants. *Nature*. 191: 493-494.

Zhao, Y., A. K. Hull, N. R. Gupta, K. A. Goss, J. Alonso, J. R. Ecker, J. Normanly, J. Chory and J. L. Celenza. 2002. Trp-dependent auxin biosynthesis in *Arabidopsis*: involvement of cytochrome P450s CYP79B2 and CYP79B3. *Genes & Development*. 16: 3100-3112.

Table 1. Hydrolases identified during BLAST analyses of the *P. patens* and *M. polymorpha* genomes and their respective accession numbers (*P. patens* accession numbers correspond with Phytozome; *M. polymorpha* accession number corresponds with GenBank)

Species	Hydrolase	Accession Number
<i>Physcomitrella patens</i>	PpIAR31	Phpat.1Z030500.1
<i>P. patens</i>	PpIAR32	Phpat.1Z047400.1
<i>P. patens</i>	PpIAR33	Phpat.1Z039000.1
<i>P. patens</i>	PpIAR34	Phpat.1Z023000.1
<i>Marchantia polymorpha</i>	MpILR1	OAE20874.1

Table 2. PCR primers utilized during the genomic DNA extraction from moss

Hydrolase	Forward Primer	Reverse Primer	Annealing Temperature
PpIAR31	5'-GCAGGAAATTGCCCTGATTA-3'	5'-CTCGACTGCCAAATAATCCA-3'	55°C/54°C
PpIAR32	5'-CGGGTGCAAAGTCGCTAT-3'	5'-AGGAAAAGCGACGGACAAG-3'	56°C
PpIAR33	5'-GGGCATGAGTACGACTTTCG-3'	5'-TAGCCGTGCCAATCTCTTCT-3'	56°C
PpIAR34	5'-AGCCGAAATCTACGGTCTGA-3'	5'-CGTCTCGGAAATCGTACTCG-3'	56°C

Table 3. Protocol specifications for endonuclease digests

Sample	DNA	H ₂ O	Buffer	BSA	Enzyme	Total
PpIAR32	7-10 µl	5-8 µl	(#2) 2 µl	1 µl	(Sall) 2 µl	20 µl
PpIAR34	4 µl	12 µl	(#3) 2 µl	1 µl	(EcoRV) 1 µl	20 µl
MpILR1	7 µl	9 µl	(#2) 2 µl	1 µl	(BamHI) 1 µl	20 µl
ΔMpILR1	1.5-2 µl	14-14.5 µl	(#2) 2 µl	1 µl	(BamHI) 1 µl	20 µl
L244SMpILR1	2 µl	12 µl	(#2) 2 µl	2 µl	(BamHI) 2 µl	20 µl

Table 4. Amino acid similarity matrix comparing percent similarity between hydrolases from cyanobacteria, algae, bryophytes, gymnosperms, monocots, and dicot species

	(1)	(2)	(3)	(4)	(5)	(6)	(7)	(8)	(9)	(10)	(11)	(12)	(13)	(14)	(15)	(16)	(17)	(18)	(19)	(20)	(21)	(22)	(23)	
(1) Cyanobacteria																								
(2) Algae	50.4																							
(3) Liverwort	47.6	59.5																						
(4) Moss 2	55.3	46	44.5																					
(5) Moss 3	54.1	46.4	44.9	77.9																				
(6) Moss 4	42	37.9	34.4	45.8	45.4																			
(7) Fern 1	53.1	54.9	60.5	49.4	49.6	41																		
(8) Fern 2	52.1	57	59.9	47.5	47.2	38	64.4																	
(9) Spruce 1	47.9	57.4	67.6	43.5	41.8	34.7	60.7	59.2																
(10) Spruce 2	47.4	56.9	66.5	41.5	41.5	32.2	60.4	60	74.9															
(11) Spruce 4	52.2	61.4	62.4	47.1	44.1	40	66.5	64.9	62.4	61.6														
(12) Spruce 3	53.3	60.8	62.6	47.8	44.8	40.2	67	65.8	66	63.9	91													
(13) Pine 1	43.7	45.5	49.5	43.5	42.6	35.6	56.3	50	66.8	55.9	53.6	56.6												
(14) Pine 2	50	53.8	57.6	43.2	43	33.9	60.3	57.9	65.5	79.9	60.7	60.5	50.2											
(15) Pine 3	43.5	45.5	50.9	42.7	42.8	34	56.5	50.5	65.7	52.9	54.5	77.3	60											
(16) Tomato	52.1	62.8	64.7	47.6	50.1	36.6	64	67.4	68.7	66.5	67.2	67.4	57.3	63.6	56.9									
(17) Tobacco	53.7	62.1	65.3	48.5	49.2	36.7	64.9	68.5	69.7	67.6	68.5	68.9	58.7	64.2	58.7	93.3								
(18) Medicago	53.7	60.9	61.6	44.7	47.7	37.6	62	64.4	66.6	66.1	65.1	66	54.6	61.3	54.1	80.3	81.9							
(19) Arabidopsis	54.1	64.1	63.3	48.4	49.5	37.3	63.4	67.7	69.1	65.5	67	67.5	57.3	60.9	54.1	79.3	82.5	81						
(20) Potato	52.6	62.8	64.3	48.1	49.2	37.8	64.3	66.3	69.1	67.1	67.2	68.1	57.8	63.1	57.1	97.3	93.5	81.4	81.1					
(21) Barley	54.4	60.8	63	47.8	49.9	38.3	65.5	68.3	68.1	66.5	68.5	68.3	57.8	64.6	56.5	77.3	80.3	74.5	77.3	78.2				
(22) Rice	46.9	46.6	46.6	44.5	43.3	35.6	54.1	51.4	51.3	49.9	53.1	52.2	54	56.5	49	58	58.5	55.3	57.7	58.4	66.9			
(23) Wheat	55.1	60.1	63.9	47.8	49.2	38.2	66.4	68.6	67.9	66.3	68.6	68.2	57.9	65.2	56.1	78.9	80.5	75.4	78.9	79.8	96.1	66.4		
(24) Corn	53.1	60.2	63.5	46.2	46.9	36	64.4	67.1	66.8	67.6	66	65.6	55.3	62.2	55.3	77.8	78.4	73.6	77.1	78.4	88.7	65.8	88.2	

Table 5. Quantification of hydrolase activity via high pressure liquid chromatography (measured in pmol auxin released/min/ml; the values recorded are the average of 3-6 assays, plus or minus the standard error)

Substrate	PpIAR32	PpIAR34	MpILR1	Δ MpILR1	L244SMpILR1
IAA-Alanine	0	313.3 \pm 11.7	0	0	0
IAA-Glycine	0	0	0	0	0
IAA-Aspartate	0	0	0	0	0
IAA-Leucine	0	234.4 \pm 64.7	10.2 \pm 5.1	0	16.23 \pm 6.29
IAA-Isoleucine	0	446.9 \pm 138.7	0	0	16.53 \pm 6.65
IAA-Valine	0	N/A	0	0	0
IAA-Phenylalanine	0	322.7 \pm 64.0	0	0	0
IBA-Alanine	0	2043.7 \pm 263.1	0	0	744.58 \pm 134.87
IPA-Alanine	0	0	1.66 \pm 1.65	0	18.32 \pm 16.69

Table 6. Copy number comparison shows the amount identified hydrolases across species of dicots, monocots, gymnosperms, and bryophytes. Numbers appearing with an asterisk* denote putative hydrolases which have not yet been fully characterized.

Plant group	Species	Identified hydrolases
Dicot (Angiosperm)	<i>Vitis vinifera</i>	15*
	<i>Glycine max</i>	12*
	<i>Lycopersicum esculentum</i>	7*
	<i>Solanum tuberosum</i>	7*
	<i>Arabidopsis thaliana</i>	7
	<i>Medicago truncatula</i>	5
Monocot (Angiosperm)	<i>Zea mays</i>	11*
	<i>Oryza sativa</i>	9*
	<i>Hordeum vulgare</i>	7*
	<i>Triticum aestivum</i>	3
Gymnosperm	<i>Picea sitchensis</i>	4
	<i>Pinus taeda</i>	4*
	<i>Picea glauca</i>	2*
Bryophyte	<i>Physcomitrella patens</i>	4*
	<i>Marchantia polymorpha</i>	1

Figure Legends

Fig. 1 Auxin is represented by several different chemical structures including **A.** indole-3-acetic acid, **B.** indole-3-propionic acid, and **C.** indole-3-butyric acid

Fig. 2 Theoretical cladogram suggested by Sztein et al. (2000) which proposes the evolution of auxin metabolism

Fig. 3 Construction of the PpIAR32, PpIAR34 and MpILR1 hydrolase inserts into expression vectors **A.** NeoScientific Labs constructed a pUC57 plasmid containing our PpIAR32 moss hydrolase insert (DNA sequence shown). The insert was ligated into the BamHI site of the pUC57 plasmid, and then re-cloned into the pETBlue-2 expression vector at the EcoRV site. **B.** Our PpIAR34 moss hydrolase insert (DNA sequence shown) was constructed with a T7 promoter and ligated into the BamHI site of a pUC57 plasmid. **C.** Our MpILR1 liverwort hydrolase (DNA sequence shown) was also constructed with a T7 promoter and ligated into the BamHI site of a pUC57 plasmid.

Fig. 4 Phylogenetic analysis of our newly identified bryophyte hydrolase genes **A.** Phylogenetic tree constructed by Skibitski (2016) focusing on the relationships between the moss hydrolases PpIAR31, -32, -33, and -34, and other previously identified hydrolases originating from gymnosperm and angiosperm species. **B.** Phylogenetic tree focusing on the relationships between the liverwort hydrolase MpILR1 and other previously identified hydrolases originating from algal, fern, gymnosperm, and angiosperm species. All alignments were created using CLUSTAL X, and phylogenetic trees contain 1000 bootstrap replicates. Bootstrap values below 500 are not listed.

Fig. 5 Principal coordinate analysis based on codon usage. Analysis was performed using the PpIAR3 hydrolase family within archaea, eubacteria, bryophytes, gymnosperms, monocots, and dicots. **A.** The two-dimensional plot representing the data was created using *ggplot2*, and **B.** the three-dimensional plot was created using CAR. **C.** Principal coordinate analysis based on codon usage was repeated, taking into account the MpILR1 liverwort hydrolase. A three-dimensional plot was created using CAR. (J. V. Smalley, unpublished method, 2016)

Fig. 6 Genomic DNA was extracted from a sample of dried moss tissue and analyzed for the presence of the **A.** PpIAR31, **B.** PpIAR32, **C.** PpIAR33, and **D.** PpIAR34 hydrolase genes through gel electrophoresis. In each of the gels, lanes 1 and 6 contained the hi-lo marker, lanes 2 and 4 contained the experimental samples, and lanes 3 and 5 contained the control samples that utilized the universal 18S primers.

Fig. 7 Endonuclease digests were performed and analyzed using gel electrophoresis, to ensure correct construction of the **A.** PpIAR32, **B.** PpIAR34, **C.** MpILR1, **D.** Δ MpILR1, and **E.** L244S-MpILR1 hydrolase inserts. In each of the gels, the first and last lanes were utilized for the hi-lo marker, and the lanes in between contained the DNA contents from

the reaction tubes (a differing amount of reactions were prepared for each hydrolase, based upon colony selection during bacterial transformation).

Fig. 8 High pressure liquid chromatography (HPLC) of a Nova Blue uninduced negative control sample (left) and an MpILR1 induced experimental sample (right). Peaks (left to right) denote DNA, hydrolyzed IAA (absent left), and amino acid auxin conjugate (IAA-Leucine).

Fig. 9 Five conserved M20D metallopeptidase domains observed across liverwort, gymnosperm, and angiosperm hydrolases

Fig. 10 Cladogram proposing the ancestry of our newly characterized moss and liverwort auxin amidohydrolase genes

Fig. 11 Structure of MpILR1 (left) and Δ MpILR1 (right) generated by SWISS-MODEL. The black arrow above MpILR1 shows the location of the extra 11 amino acid sequence. The black arrow above Δ MpILR1 shows the absence of the extra 11 amino acid sequence. The white arrows in both images show the location of the active site in each structure.

Fig. 1

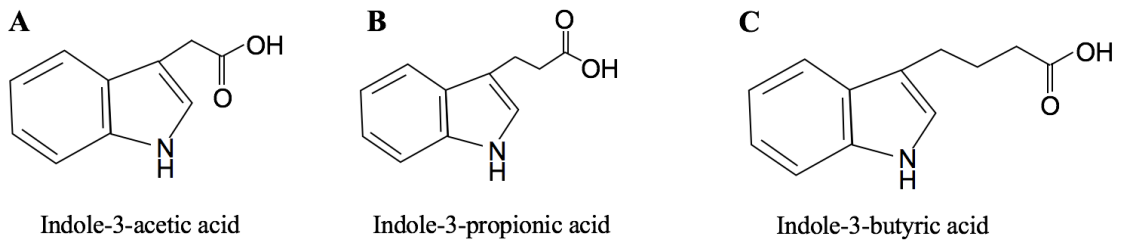


Fig. 2

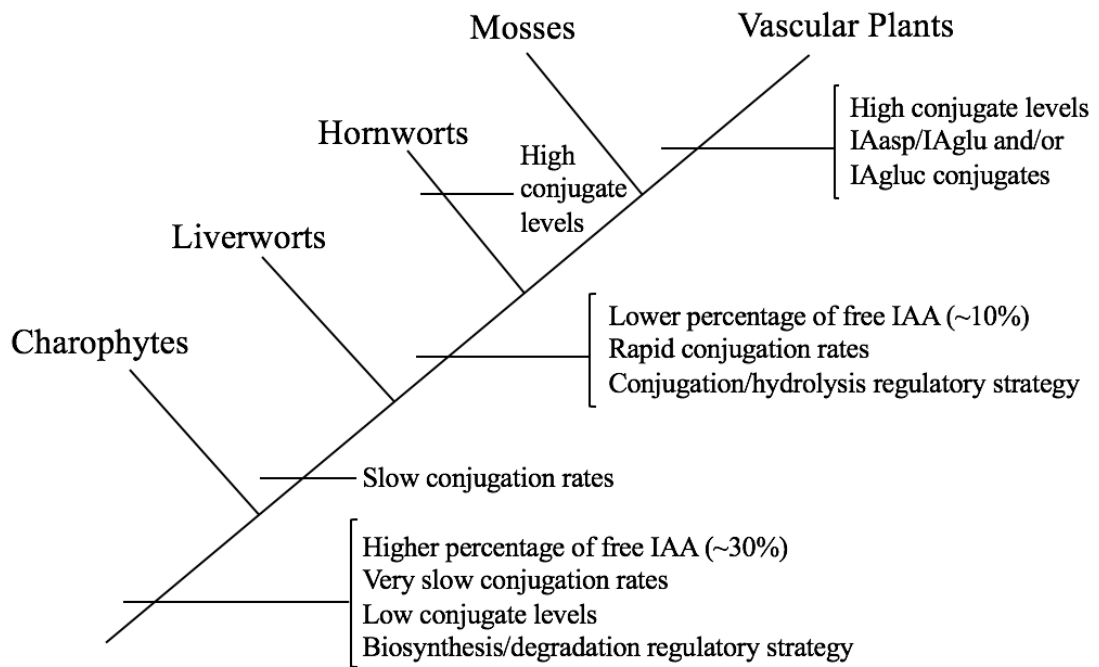
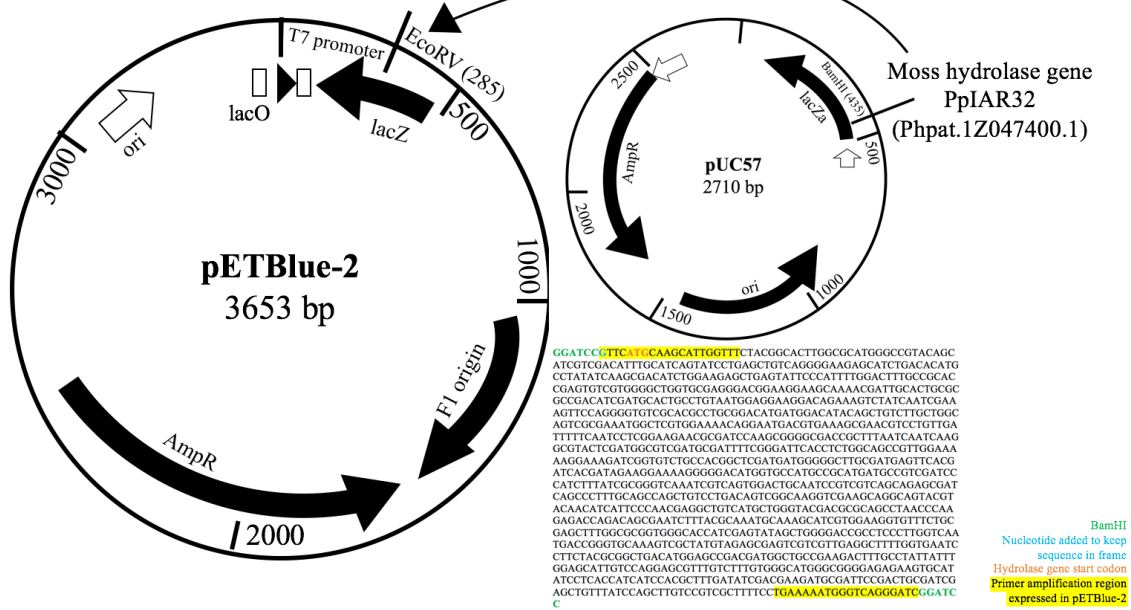
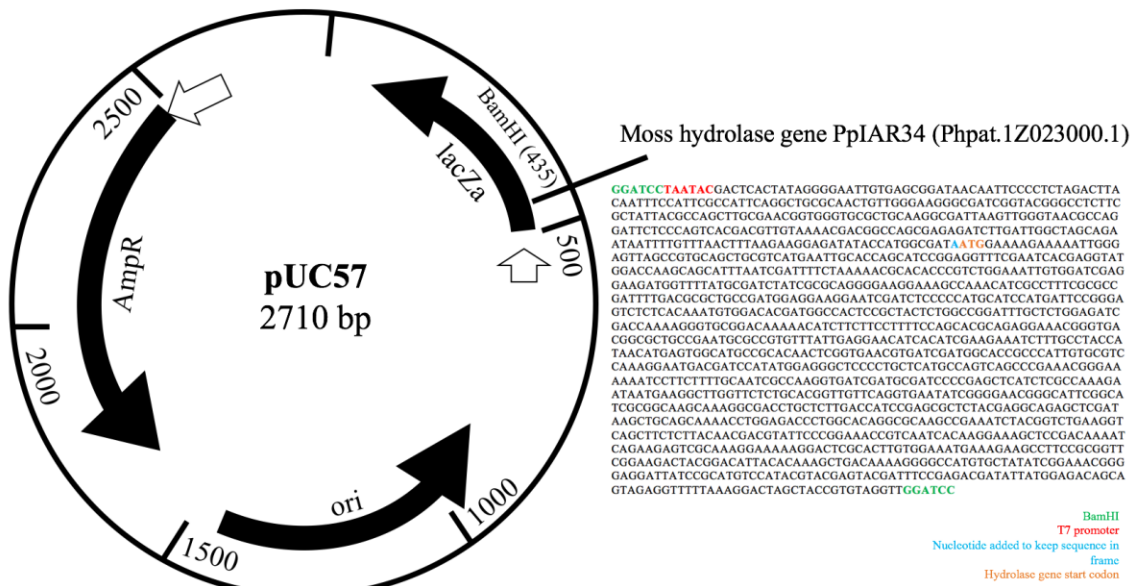


Fig. 3

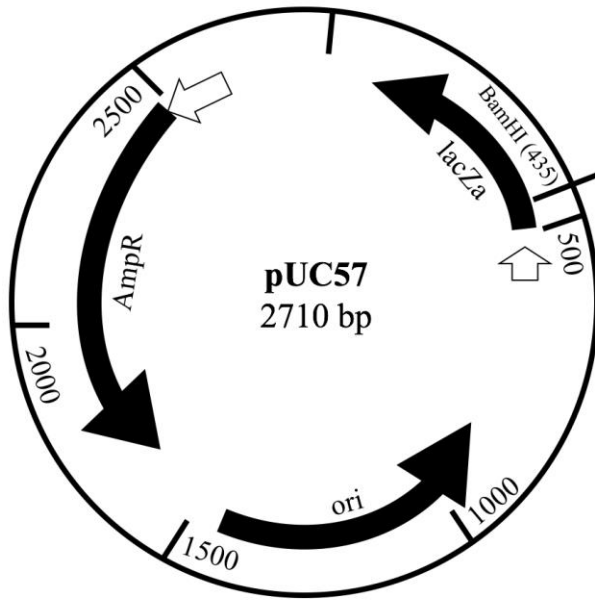
A



B



C



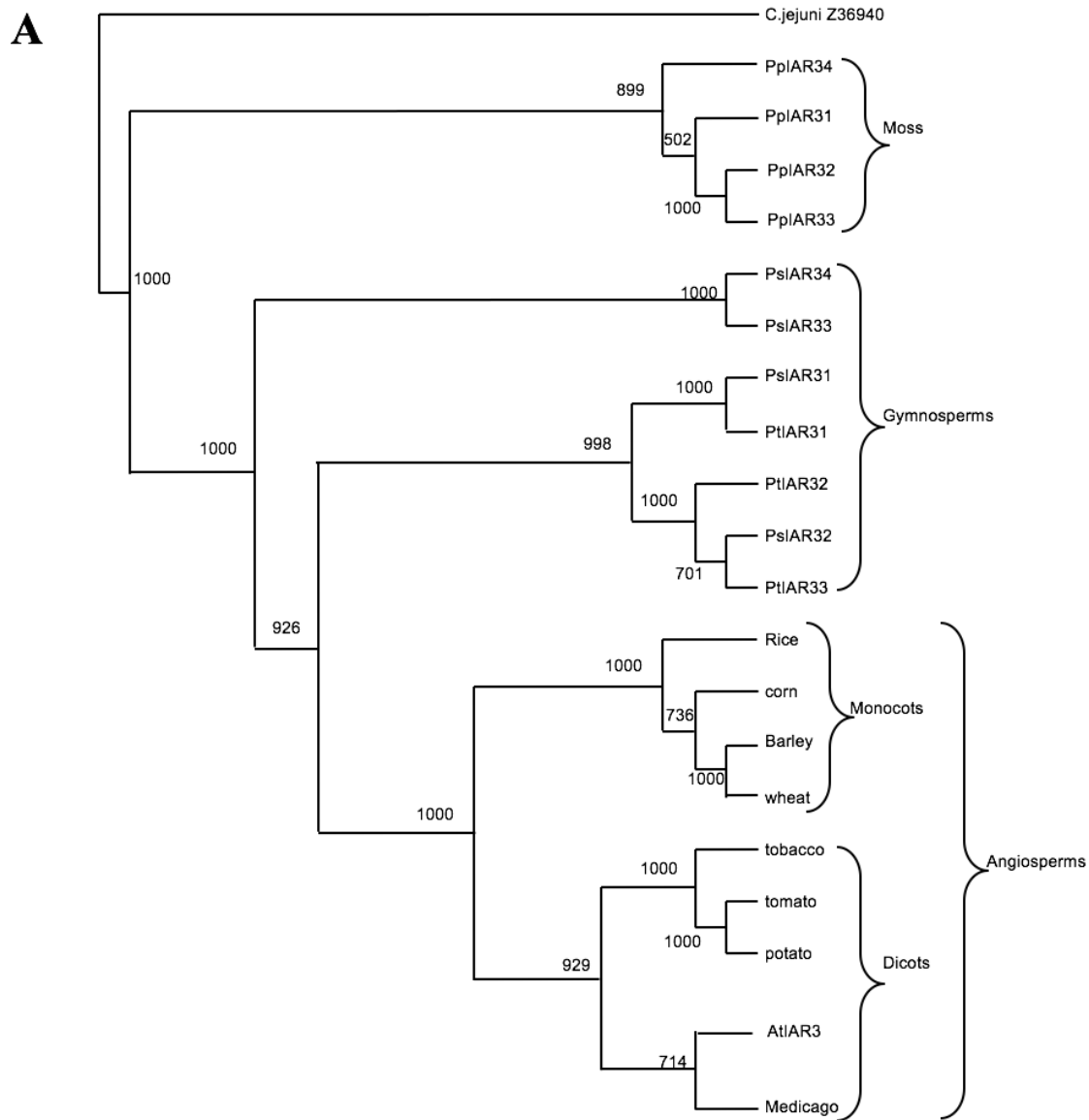
Liverwort hydrolase gene MpILR1 (OAE20874.1)

```

GGATGCTAATACGACTCACTATAGGGGAATTGTGAGCGGATAACAATTCGCCCTTAGACTTACAATT
CCATTGCCATTACGGCTGGCAACTGTTGGGAAGGGCGATCGGTACGGCCCTCTGGCTATTACGCC
AGTTGGCAACGGTGGGTGGCTGCAAGGGGATTAAGTTGGTAAACGCCAGGATTTCCACGTCACGA
CGTTGTAAACGACGGCCAGCGAGAGATCTTGATTGGCTAGCAGAATAATTTGTAACTTAAAGAA
GGAGATATACCATGGCGATAATGAGCGCCGAGCATGATGGCTACAGCCGAGGCTTGGCCATGCT
ACTTGGCTGAGCGCTGTTCTTTGGCGGTCTGGCGAAGCCGCTAGTGTGAGTCTACGCTGCTGCC
CGGCTCTCTGCGCCGTGGAGTTGGCGCTCCGCCAAGGCCCGACGAGGAGAATGTAATAGTGTGA
TCGGCGTGCAGCCACAGTCCGACATGATCGAATGGTCCAGACGACCTCCGCTATCTGCACTGG
CATCCGGAATTGTCATGGCAAGAATTCGAAACAGTGGTTTCATTCCGAAGCAGTGGACTCGCTGGG
CATTCGCTACGAGTGGCCCGTGGCCAAGACCGGCTCGTGGGTAATTTGGTCCGGGAATGGCCCTT
GTATCGCTCTCCGCCCGACATGGAAGCTCTCCCGATTCAAGGAGGAAGCCGAGCCAAAGCATCCGAGC
TAAATGCCGCCGAATGCACGCTGCGGGCACGACGCGCATGTACACCTCTGCTGGGGTTGCCAA
ACTTTCGAAGTCTCGCGCACCTCATTCTCTGTAAGTCTCGAACATTACAGCCACAGGCGTGGG
GACGATAAGTTGGTATTTCAACCGGCAGAGGAAGGCAACCGCGGGCTCAGGTGATGGTAGAGAAG
GGGCCCTGGGAACCGTGAAGTCTATTTGGATTACACGTTACGCCGTTCTCAGAACTGGAAACCGTC
GCACATAAAGCCAGGGCCCTCATGGCAGGAGTGGCAATTCGAAGCTCTGATCATGGCAAGGAG
GCCATGCCGCTGCGCAGCTGCTACCGATCCATCTCGCTGCCCAACCGCATCGCCGCTG
AGCAGTGGTGGCGCGAGCCGATCCTTTGGATTCTCAGGTGCTCGGTGAGCATTTCGCAAGG
GGCAAAGCGTACAACGTGTGCCGACACAGTGGCTGGCGGAACCTTCGAGCTTCTCTCTGGA
GAGCTCCGAAGGCTCAAGCAAAGAATTGAGGAGTAAATTTGACACAGGCTGCGGTGATAAGTGC
GCAGCCACTGTGACTTCACTGAGGACTGGATCATTTACTATCCGCCGACAAATAATGAGAAAGCT
GTATGAGCAGTGCATGGAGTGGCGTGGACATGCTGGGCAAGACAAAGGTGTGTGAGCGATCCG
GTATGGGGGCGGAGGATTTCCGCTTACTTTGGCAAAAATCCAGGGTTCTACATGCTGCTGGGAT
GAGAAATGTGAGCTACGGTTCGACGTTTCCGGGCACACCTCGCGCTTCTGGTGGATGAAACATGCGC
TGCCGTATGGGGTGTGGTCAATGGCTGGCTGGCCGAAACGATATCTGAAGAAATGGATTCTCAACGA
AAAAGGCGGGCAGAGGGGATCAGTGCATGCTATATACAGTGCACACCACCCACCCACTAA
GGATCC
    
```

BamHI
T7 promoter
Nucleotide added to keep sequence in frame
Hydrolase gene start codon
Sequence deleted in ΔMpILR1
Codon changed to "TCA" in L244ΔMpILR1
Histidine tag

Fig. 4



B

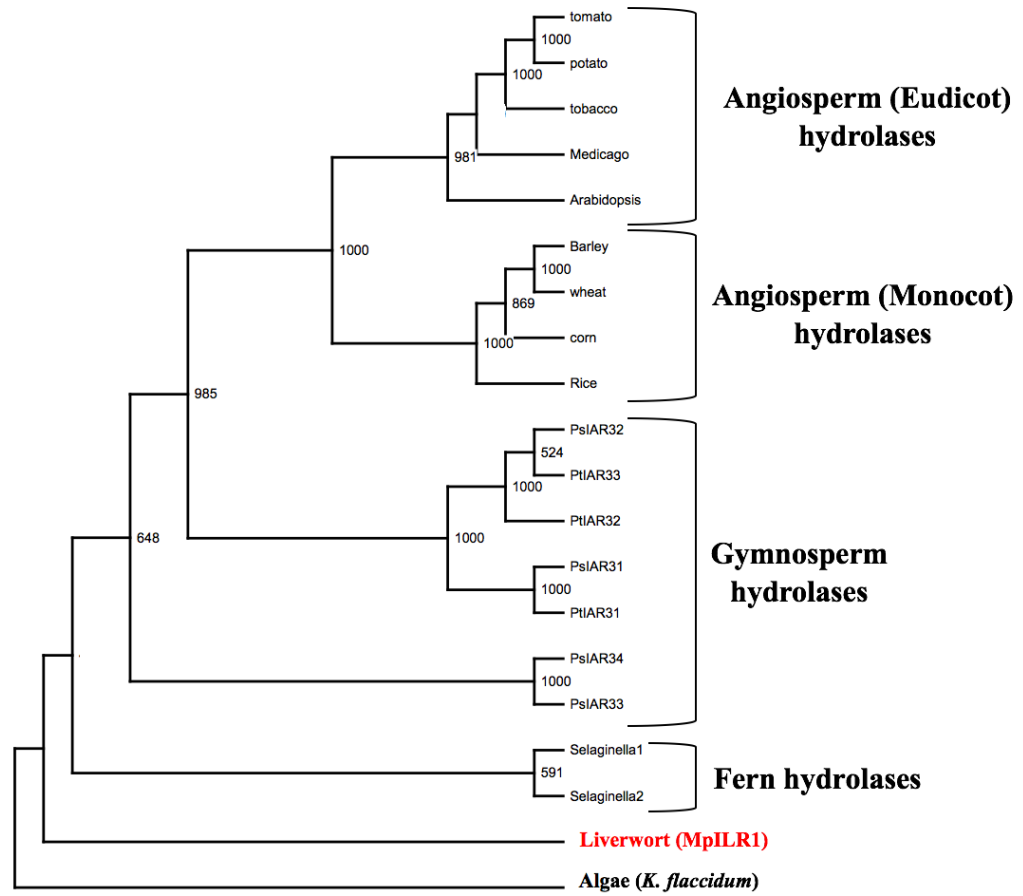
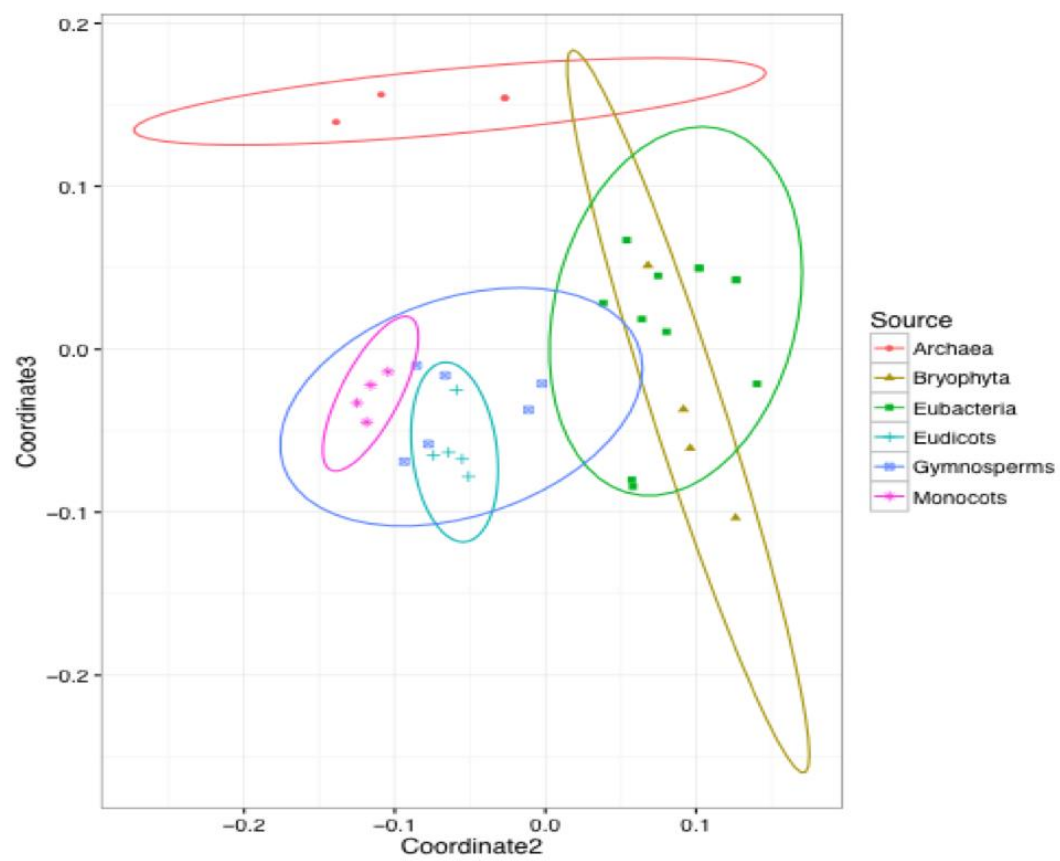
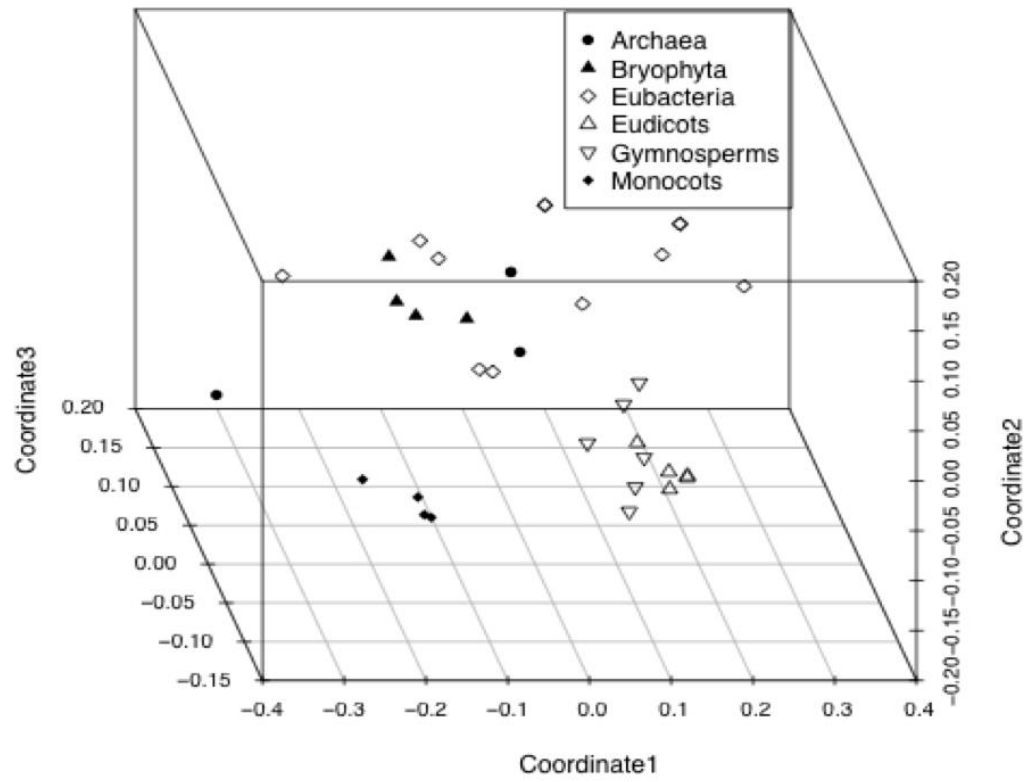


Fig. 5

A



B



C

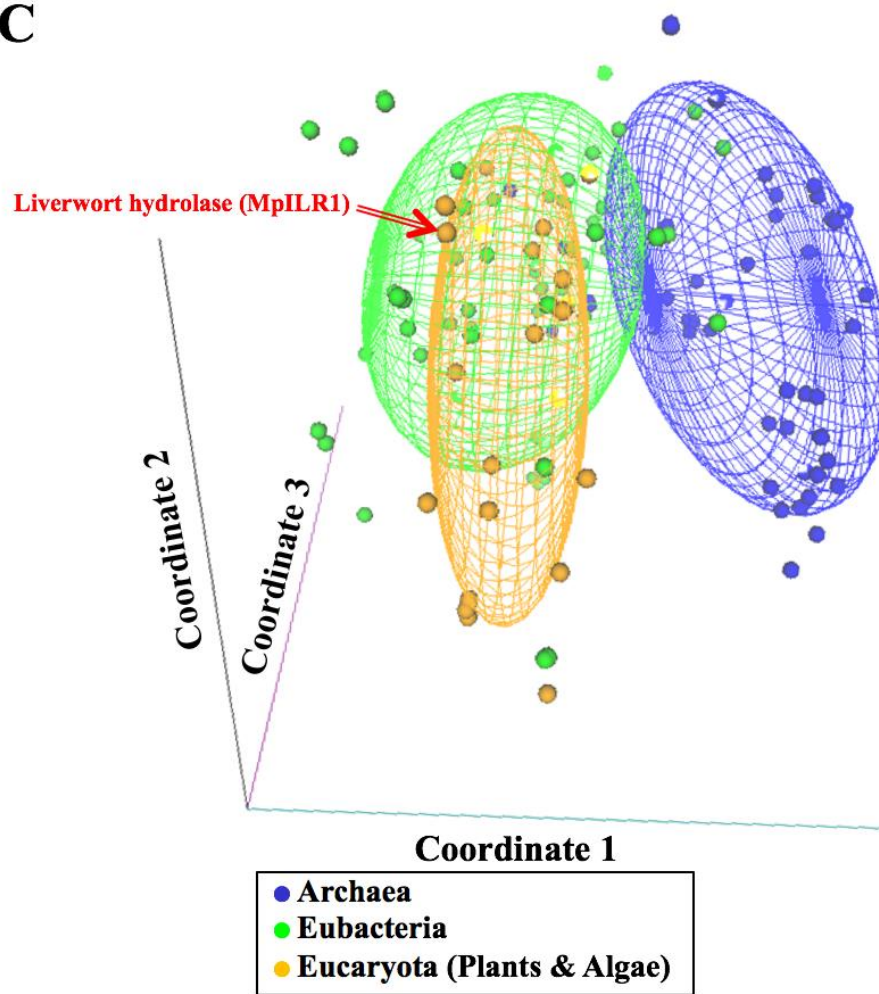
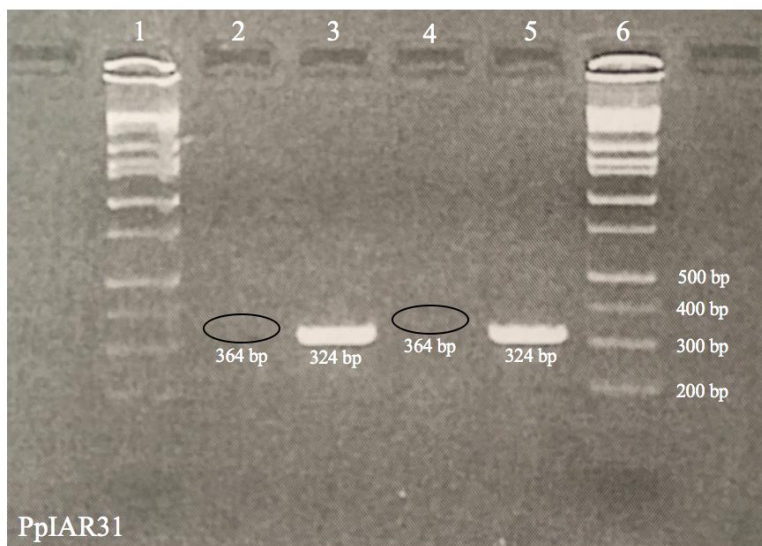
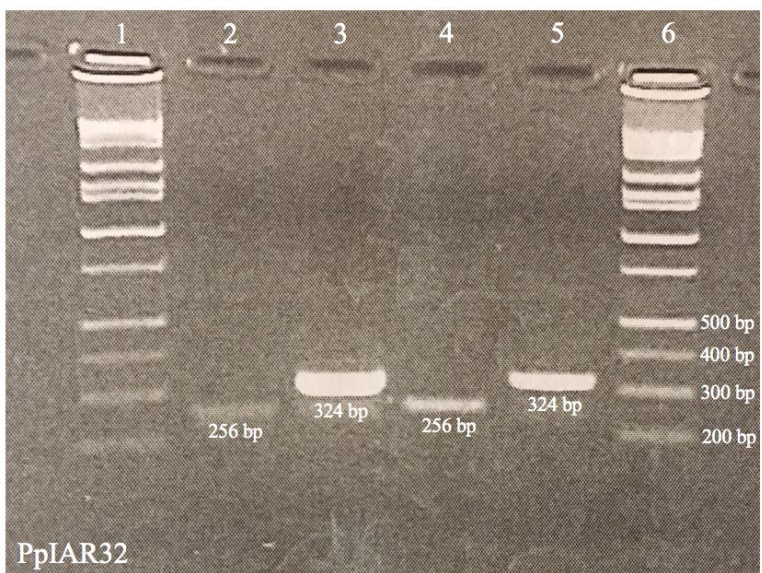


Fig. 6

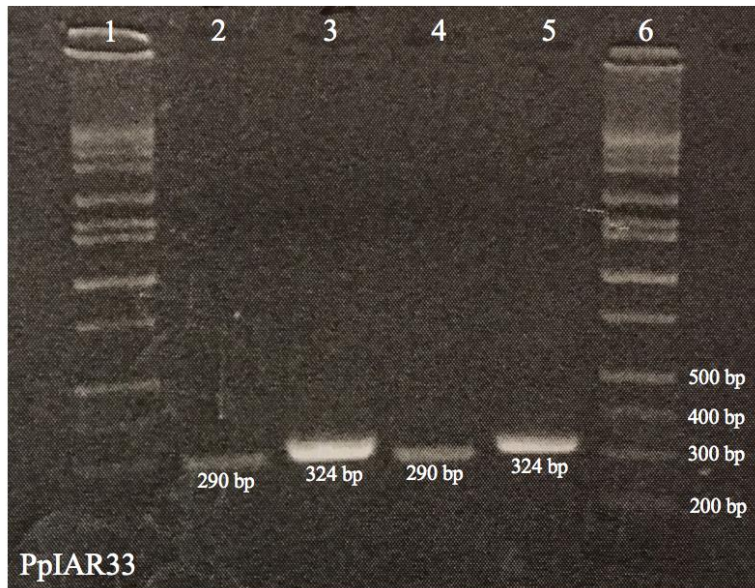
A



B



C



D

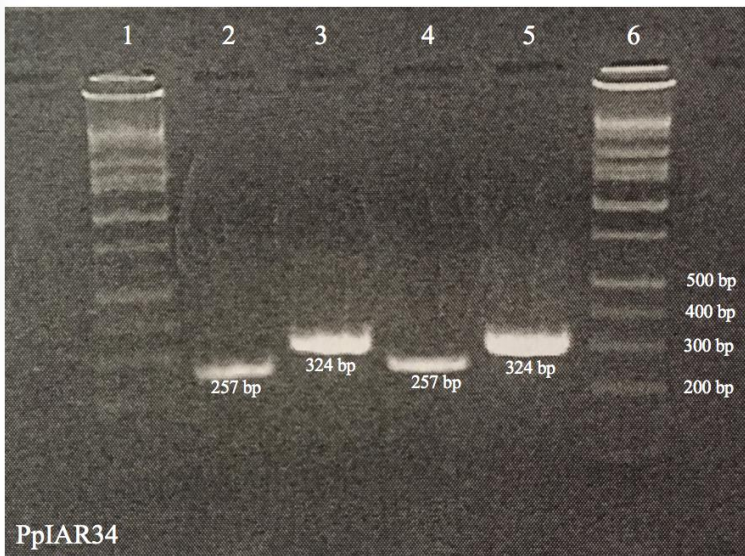
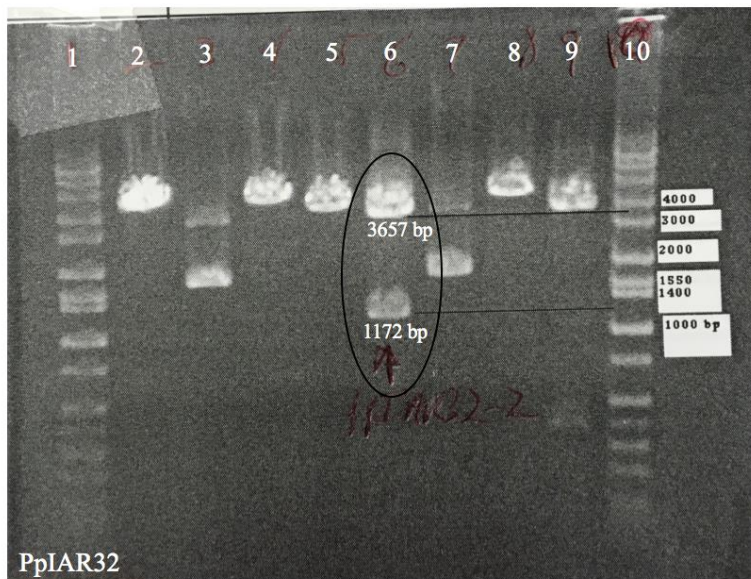
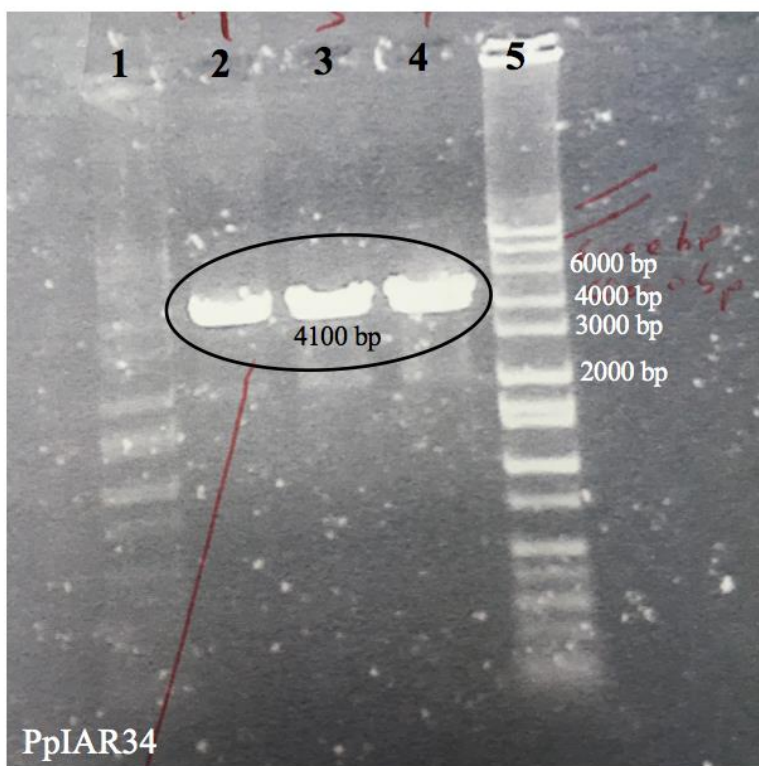


Fig. 7

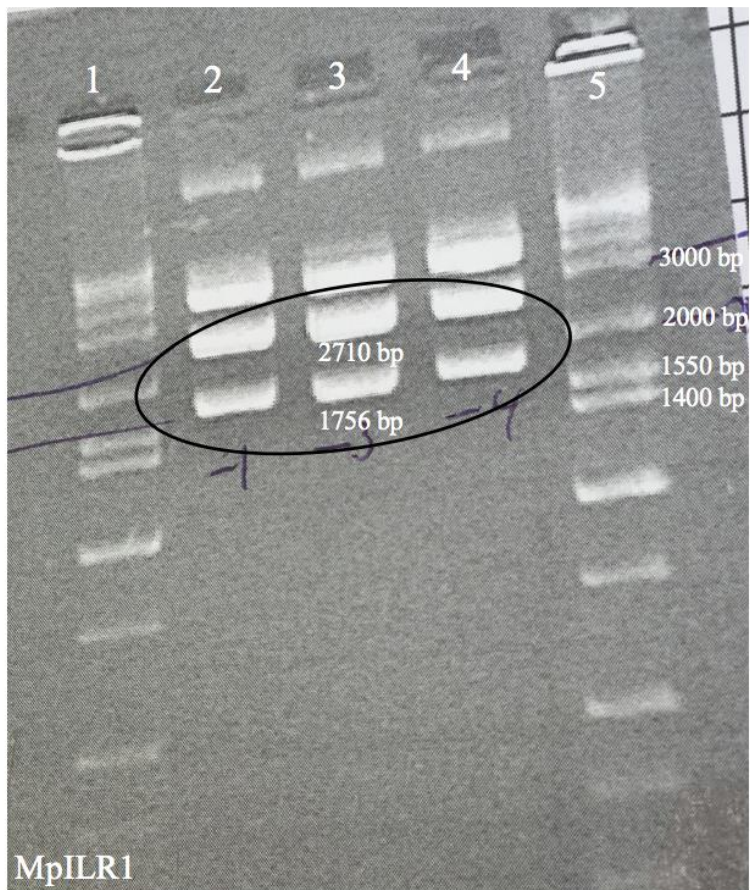
A



B



C



D



E

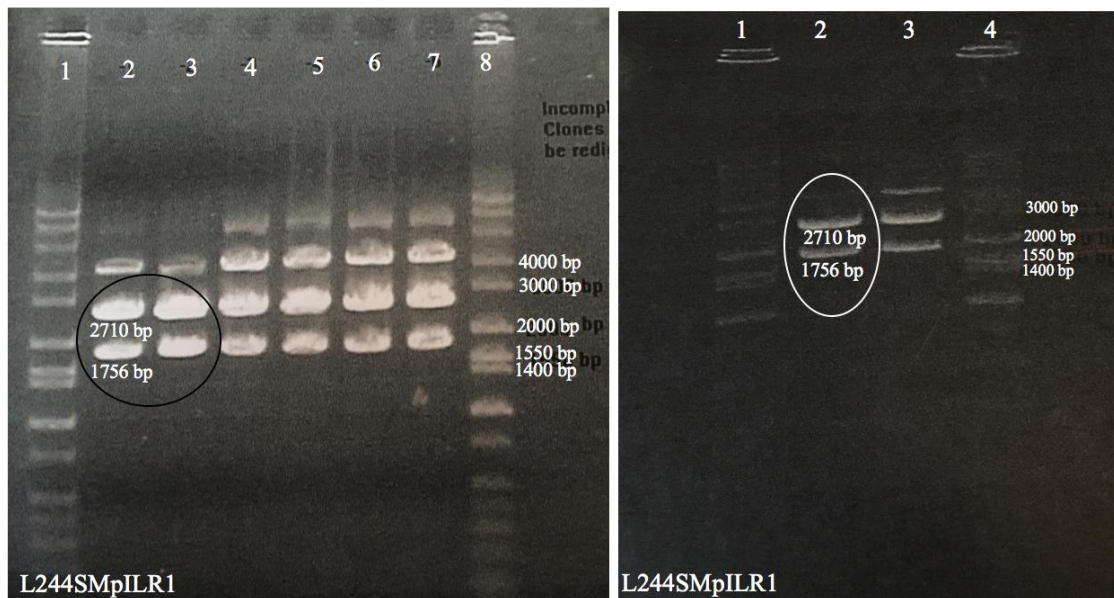


Fig. 8

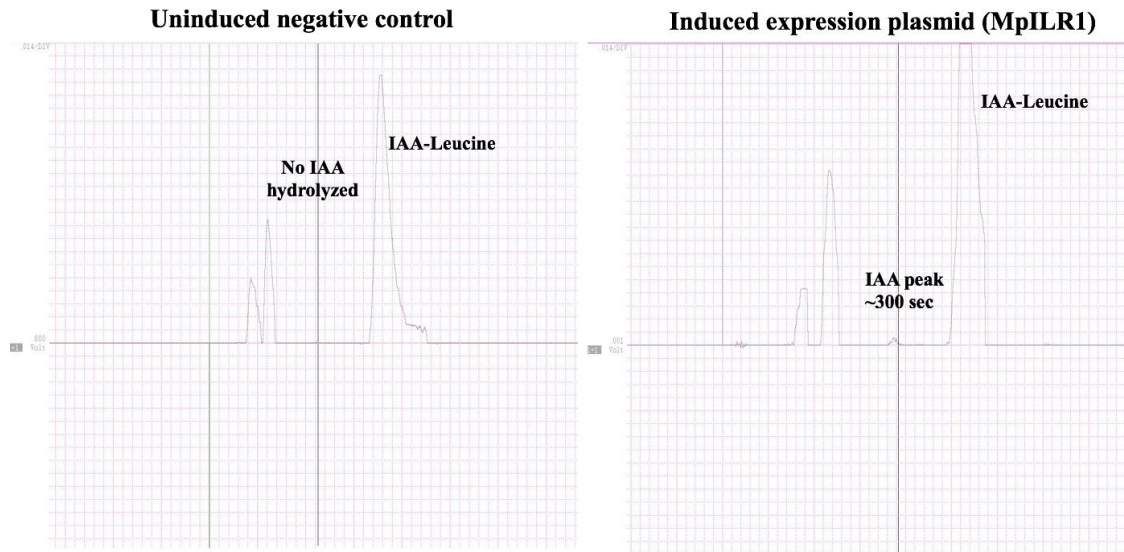


Fig. 9

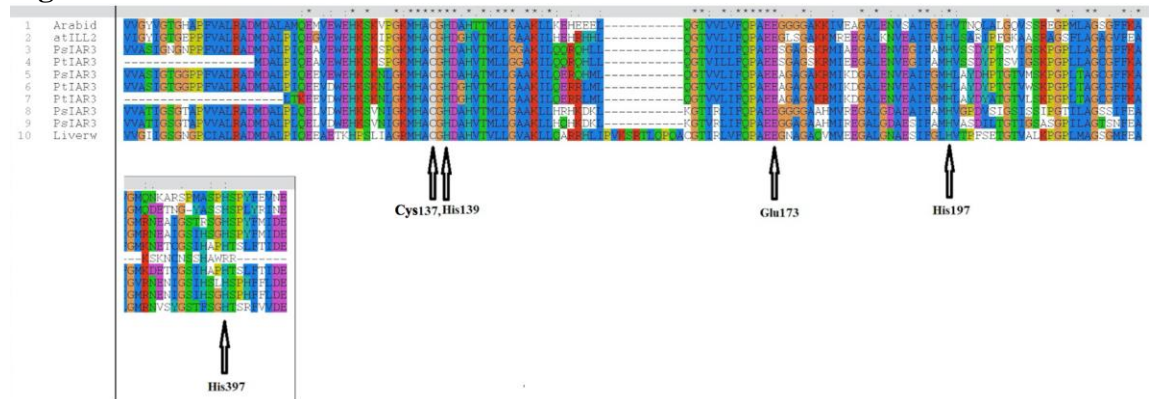


Fig. 10

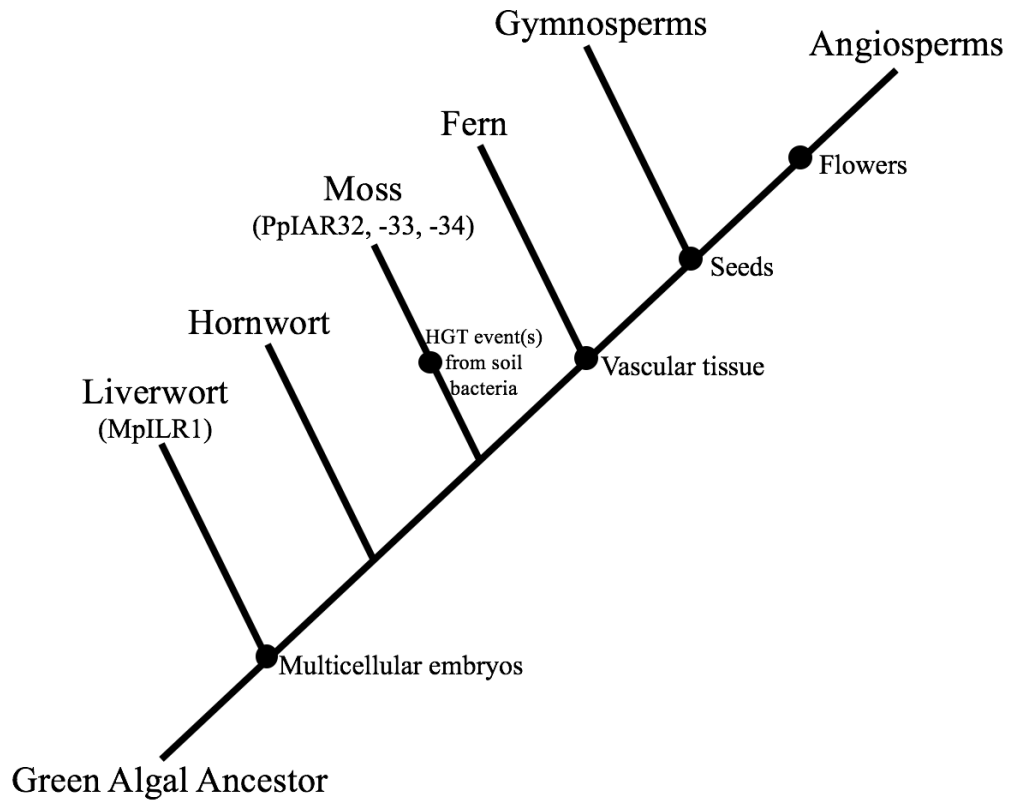


Fig. 11

